Photoisomerization Dynamics of Stilbenes

D. H. WALDECK

Department of Chemistry, University of Pittsburgh, Pittsburgh, Pennsylvania 15260

Received August 16, 1990 (Revised Manuscript Received December 17, 1990)

Contents

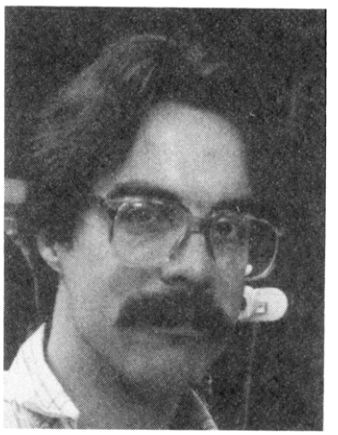

David H. Waldeck was born in Cincinnati, OH on September 5, 1956. He obtained a B.S. in chemistry from the University of Cincinnati (1978) and a Ph.D. in chemistry from the University of Chicago (1983). He was a postdoctoral fellow at the University of California, Berkeley from 1983 to 1985. In 1985 he moved to the University of Pittsburgh as an Assistant Professor of Chemistry. His research interests include condensed-phase reaction dynamics (homogeneous and heterogeneous), solute/solvent interactions (both structural and dynamical characteristics), relaxation processes in solids, and developments of nonlinear and ultrafast spectroscopies.

I. Overview

Recent developments in the understanding of stilbene photoisomerization are reviewed. Stilbene's reaction dynamics has been studied over a wide range of friction and provides a useful model system for the investigation of condensed-phase reaction dynamics.

II. Introduction

The photoisomerization of stilbene is an important model for the study of reaction dynamics in the condensed phase. It is also representative of cis/trans isomerization reactions, a class of unimolecular reactions. An important feature of the stilbene system is the ability to follow the reaction through a range of environments, from the isolated molecule to gas-phase densities and into the liquid phase. The photoisomerization of stilbene and its simple derivatives has been studied for more than 45 years.[1-4] The study of stilbene reaction dynamics is leading to a deeper understanding of the important role that solvent plays in chemical reactions. In the past decade, new insights have been made into the role of nonequilibrium solvation and solute/solvent friction. The insight gained from stilbene dynamics has considerable use in understanding condensed-phase reactions, in general.

This review focuses on the rate studies of stilbene and its simple derivatives. The chemistry of stilbene is straightforward, which allows for the creation of many functional derivatives. This ability to tune the reactant's properties aids in the study of solute/solvent interactions and their influence on the reaction. For the trans isomer the excited reactant form lives for time scales long compared to vibrational relaxation in condensed phases. This time-scale separation allows comparisons of the measured rate to be drawn with models that assume a steady-state population of activated species, in the gas-phase RRKM, and in solution Kramers type models. Conversely for the cis isomer this time-scale separation may not be possible because of the rapid isomerization rate. The dynamics in this regime can be used to test non-steady-state models. This complementary behavior in structurally similar molecules makes stilbenes interesting test systems.

The presently accepted (one-dimensional) potential energy scheme for the isomerization of stilbene is represented by the sketch in Figure 1 and was proposed

0009-2665/91/0791-0415$09.50/0

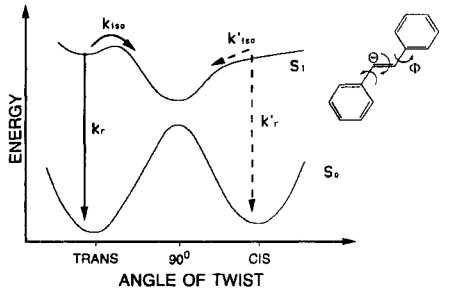

Figure 1. A schematic representation of the isomerization coordinate is shown for reaction from both the trans and cis sides. The rate constants k_{iso} and k'_{iso} are for isomerization on the singlet surface and the rate constants k_r and k'_r are for radiation.

in 1967.[5] The reaction coordinate corresponds to a large amplitude motion of the phenyl rings and presumably involves a large amount of ethylenic torsion. In the ground electronic state a large barrier exists between the trans and cis forms of stilbene. In the first excited state of *trans*-stilbene there is a potential minimum and a barrier exists for the twisting motion about the ethylene bond. On the cis side there appears to be little or no barrier to torsional motion. The surface sketched here arises from a mixing of the first excited B state (obtained by a $\pi \rightarrow \pi^*$ transition) of stilbene with one or more higher lying, doubly excited configurations that have a minimum at the 90° twisted form. This sketch corresponds to the adiabatic limit. Because of the nature of the higher lying states, the 90° form and the transition state are expected to be polarizable (both biradical and charge-transfer structures have been proposed[2,6,7]). After the *cis*- or *trans*-stilbene arrives at the twisted form (90°), the decay to the ground-state surface is rapid (<1 ps in liquid alkanes). Once on the ground-state surface the product molecule branches to either the trans or cis form. A third reaction channel, believed to be minor, is open from the cis side and produces dihydrophenanthrene (DPH). The justification for this view of the reaction will become apparent as the discussion proceeds.

This review has four major components. First, the recent surge of activity on the spectroscopy, both gas phase and solution phase, of stilbene is discussed. Second is an overview of stilbene photoisomerization from a mechanistic perspective. This treatment will be somewhat cursory, since reviews are available. Next, relevant theoretical models are outlined. The fourth and primary discussion concerns the rate studies in dense gases and liquids. The discussion concludes with a statement about present and future questions.

III. Spectroscopy and Structure

The spectroscopy of stilbene and its analogues is becoming clear. The development of laser methods and supersonic beams has made the spectroscopy of the trans isomer accessible. Progress is being made in understanding the cis isomer, but it remains a challenge.

The electronic state manifold of stilbene has consumed the efforts of numerous theoretical[7-13] and experimental groups.[14-17] A commonly used model for the isomerization of stilbene in the first excited singlet state involves coupling to higher excited states and was proposed by Orlandi and Siebrand.[8] In this model, the initially excited B state (S_1) has a minimum for the trans configuration of stilbene and the energy increases monotonically as the angle about the ethylene bond increases. This state is believed to cross with a doubly excited configuration which is decreasing in energy as the angle of twist evolves from the trans value to the 90° form. This doubly excited state has a minimum at 90° (the "phantom" state[5]) and correlates with the ground state of the cis form. Correspondingly the ground state of the trans form correlates with the doubly excited configuration of the cis form. Whether this doubly excited state is the lowest lying A state is not clear.[16]

TABLE I. Inertial Constants for *trans*-Stilbene[a]

state	constant	experiment	QCFF/PI, MHz
^1A_g	A''	2611.3 ± 7.7 MHz	2659.1
	B''	262.86 ± 0.02 MHz	261.6
	C''	240.56 ± 0.02 MHz	238.2
	κ''	−0.9812	
	$\Delta I''$	−15.3 ± 0.6 amu Å^2	
^1B_u	ΔA	−71.14 ± 0.06 MHz	−61.0
	ΔB	5.928 ± 0.004 MHz	2.8
	ΔC	3.963 ± 0.005 MHz	1.8
	$\Delta\kappa$	0.0023	
	$\Delta(\Delta I)$	2.9 ± 0.9 amu Å^2	
	band origin	32234.744 ● 0.02 cm^{-1}	

[a] Reproduced from ref 18.

A. Jet Studies

The trans form of stilbene with no excess vibrational energy is planar in both the ground and excited states. This conclusion is drawn from two primary sources. Measurement of the rotational contour of the zero-point vibrational level of stilbene with <1 MHz resolution[18] allows the rotational constants of the molecule to be measured (see Table I). It is found that a rigid-rotor model fits the spectrum well and the moments of inertia place strict constraints on the geometry. It is also concluded that the transition moment lies within 12° of the long axis of the molecule (*a* axis). Second is the assignment of the vibronic structure of stilbene,[19-24] in particular the low-frequency modes, which indicates a point group symmetry of C_{2h}.

A complete assignment of the vibronic transitions has recently been reported by Hamaguchi.[19] Of the 72 vibrational degrees of freedom 25 are a_g (in-plane, in-phase), 12 are a_u (out-of-plane, out-of-phase), 11 are b_g (out-of-plane, in-phase), and 24 are b_u (in-plane, out-of-phase). The mode assignments and characteristic frequencies for the first excited state are given in Table II for those modes active in the excitation spectrum. These assignments were made through the use of ^{13}C and deuterium labeling, and the assignments of different workers are generally in agreement. The frequencies of the corresponding ground-state modes are also given in the table.[23-26] The modes of probable importance to the isomerization are those associated with the ethylenic moiety (ν_{24}, ν_{25}, ν_{27}, ν_{33}, ν_{35}, ν_{45}, ν_{72}) and, possibly, other low-frequency modes (ν_{36}, ν_{37}, ν_{48}). In this assignment,[19] the stretching frequency of C_e–C_e (Note: C_e is an ethylenic carbon) decreases from 1639 cm^{-1} in the ground state to 1551 cm^{-1} in the excited state and the associated shift in the phenyl ring C–C stretch is consistent with excitation of an electron from the ethylenic π orbital to a π^* orbital of the ring system.

TABLE II. Vibrational Mode Assignments for *trans*-Stilbene[a]

mode	mode description	S_0 cm^{-1}	S_1, cm^{-1}
	a_g Vibrations		
7	C=C stretch	1639	1551
8	ring stretch	1598	1533
9	ring stretch	1577	
10	ring stretch	1491	
12	ring str + CH def	1337	1333
13	olefinic CH def	1322	(1244)
14	ring str + CH def	1315	1269
15	C-phenyl str	1194	1162
16	CH def	1182	1157
17	CH def	1157	
18	CH def	1059	1069
19	CH def + ring def	1028	993
20	trigonal + breathing	999	970
21	ring def + C=C-C def	854	(849)
22	ring def	641	621
23	ring def	619	588
24	C-C_e def	293	276
25	C=C-C def	202	199
	a_u Vibrations		
27	C_eH def	963	
33	C-C_e def	526	418
34	ring tor	455	358
35	C=C tor	268	276
36	skeletal tor	<60	46
37	skeletal tor	8	34
	b_g Vibrations		
45	C-C_e def	410	410
46	ring tor	338	331
47	ring tor	239	248
48	skeletal tor	114	(114)
	b_u Vibrations		
72	C=C-C def	262	99

[a] Adapted from refs 19b and 23–26.

This assignment has been challenged by Saltiel[1,2] on the grounds that such a frequency is inconsistent with the reduction of the torsional barrier. Clearly this mode is not pure ethylenic stretch; however, deuterium and ^{13}C isotope studies indicate that it has significant ethylenic stretch character.[11,27,28] A recent force field analysis[11b] indicates a larger decrease in the ethylene stretch frequency than is given in the previous assignment, and a corresponding increase in the C_e–phenyl stretch frequency, such that the force constants for these vibrations are similar in S_1. The rotational analysis[18] is consistent with this force field analysis and can be used to estimate bond length changes. It is found that the C=C length increases from 1.36 Å in the ground state to 1.44 Å in the excited state, indicating that the central bond retains double bond character similar to that found in aromatic compounds. The C_e–phenyl bond has a corresponding decrease in bond length from 1.48 Å in the ground state to 1.42 Å in the excited state. The loss in double bond character of the ethylene moiety is consistent with a reduction in the activation energy for ethylene torsion which allows isomerization. Although this frequency is lowered, it is significantly greater than a single bond frequency (993 cm^{-1} for the C–C stretching frequency of ethane[29]). Also, the low-frequency modes apparent from the assignment in Table 2 will be excited at room temperature and could be important to the detailed description of the isomerization dynamics.

The fact that stilbene is planar under ultracold jet conditions and in the crystalline solid[30] places constraints on gas- and liquid-phase structures. However, a variety of observations indicate that the presence of low-frequency out-of-plane modes (ν_{37} and ν_{36}) could lead to large excursions from the planar geometry. Both electron diffraction[31] and photoelectron spectroscopy[32] studies conclude that the C_e-phenyl torsional angle (Φ) can be quite large. Probing ground-state stilbene in a supersonic jet expansion, Suzuki et al.[23] find the ν_{37} mode to be very anharmonic and shallow. Their observations are consistent with the potential function

$$V(\Phi) = V_2(1 - \cos 2\Phi)/2 + V_4(1 - \cos 4\Phi)/2$$

where $V_2 = 305$ cm^{-1} and $V_4 = -85$ cm^{-1}, which leads to a barrier for ring flipping of 305 cm^{-1}. In the excited state this barrier increases significantly, perhaps to a value near 750 cm^{-1}.[33,34] A recent theoretical study by Fredericks et al.[35] indicates that this barrier may be of the order of 1500 cm^{-1}. These observations are also in agreement with the large amount of spectral congestion for the thermal vapor of stilbene.[36] Spectroscopic studies of stilbene in rare gas van der Waals clusters reveal significant coupling between intramolecular and intermolecular modes, in particular the low-frequency out-of-plane motions of stilbene. Lastly, the general features of the vibrational spectrum of stilbene in solids[24,25] and liquids[26] is consistent with large Φ angle excursions (30° and more).

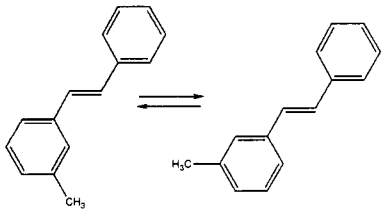

Figure 2. Molecular structures of the two interconverting conformers of 3-methylstilbene are shown.

Zwier and co-workers[34] have studied the influence of methyl substitution on the spectroscopy of stilbene. The impact on the overall spectrum is quite interesting. For 3-methylstilbene two conformers are observed corresponding to the methyl group being syn and anti of the ethylene (see Figure 2) with a shift in the zero–zero transition energy between the conformers of 207 cm^{-1}. The presence of these conformers has also been observed in the condensed phase.[37,38] For the case of 4-methylstilbene only one conformer is possible. A detailed study of the methyl rotor transitions shows that it is 3-fold symmetric, indicating that the meta positions of the ring are inequivalent. The barriers for the methyl rotor in the three species ranges from 80 to 186 cm^{-1}. Their observations indicate that the methyl rotor is coupled to the low-frequency modes of the stilbene, in particular the ν_{37} mode. Studies in van der Waals clusters also indicate the importance of the low-frequency modes for coupling intermolecular and intramolecular motions in these stilbenes.[39]

Recent studies[40] have probed the spectroscopy of the cis isomer in jet expansions. The fluorescence spectrum is broad and featureless, similar to the spectrum observed in viscous solutions.[41–43] The jet spectrum is only observed with cis in a cluster of rare gas atoms and the fluorescence intensity increases with the atomic number of the rare gas atom. The emission and long lifetime of the cis isomer (17.2 ns) in these clusters indicates a shallow minimum on the cis side. The geometry of the

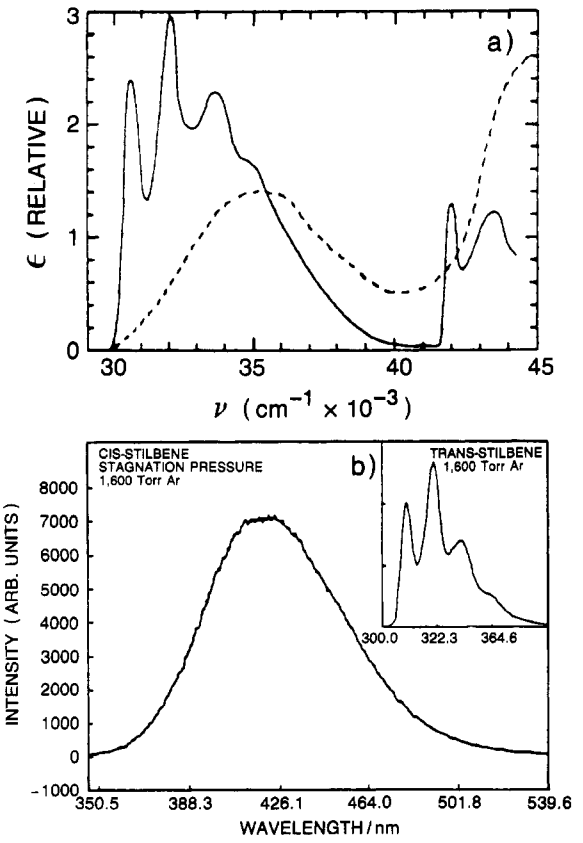

Figure 3. Low-temperature absorption and fluorescence spectra of *trans*- and *cis*-stilbene are shown: (a) the absorption spectra are taken at 77 K in methylpentanes (solid line is trans and dashed line is cis) and are adapted from ref 16 (Copyright 1984 Elsevier Sequoia.); (b) The fluorescence spectra correspond to an ultracold cluster of argon containing *cis*-stilbene and *trans*-stilbene (inset) and are reproduced from ref 40 (Copyright 1988 American Chemical Society.).

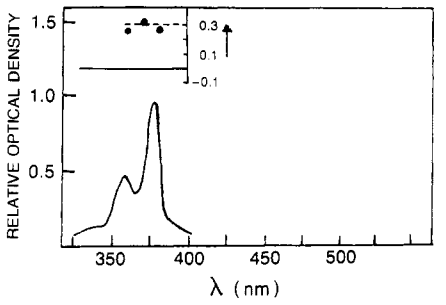

Figure 4. The triplet–triplet absorption spectrum is shown for *trans*-stilbene at 77 K and is taken from ref 48a. Copyright 1985 Pergamon.

cis excited state is believed to be nonplanar.[44]

B. Solution Studies

The solvated absorption and fluorescence spectra of *trans*- and *cis*-stilbene have been known for quite some time.[41-43,45-47] The broadening and smoothing of the cis absorption spectrum appears to be linked to its nonplanar geometry (see Figure 3). The vibronic structure preserved in the trans isomer is 1500–1600 cm^{-1} and is probably associated with C=C stretching (of both the ethylene and ring moieties of the excited state). Considerable effort has also been placed on obtaining the lowest triplet[48-52] and excited singlet state[3,53-55] spectra because of their importance in monitoring the isomerization dynamics (see Figures 4 and 5). These spectra can be distinguished by their spectral and temporal characteristics.

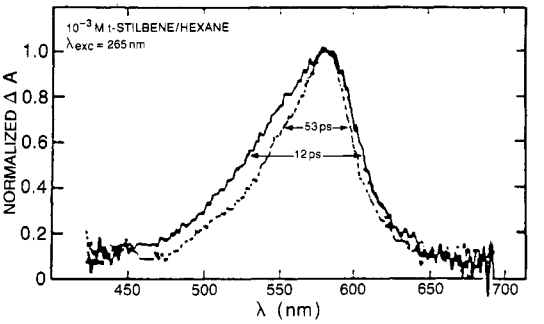

Figure 5. The excited singlet state absorption spectrum for *trans*-stilbene is shown. The change in spectral width with time results from vibrational relaxation in the excited state. Adapted from ref 53. Copyright 1979 Elsevier.

TABLE III. Electronic State Ordering[a]

assignment	symmetry D_{2h}	symmetry C_{2h}	symmetry C_2	CNDO/S[b] (SDCI/P 200 ππ*)
$-L_A + E$	B_{3u}	B_u	1B	4.67 (0.921 l)
$-L_b$	B_{2u}	B_u	2B	4.98 (0.007)
$+L_b$	B_{1g}	A_g	2A	4.98
$+L_a$	A_g	A_g	3A	5.56
$+B_a$	A_g	A_g	4A	6.04
$-B_a + E$	B_{3u}	B_u	3B	6.11 (0.31 l)
$+B_b$	B_{1g}	A_g	5A	6.48
B_b	B_{2u}	B_u	4B	6.57 (0.67 s)

[a] Adapted from ref 16. [b] l: mainly polarized parallel to long axis. s: mainly polarized parallel to short axis.

Two photon spectra in combination with polarization dependent absorption spectra of *trans*-stilbene[16] have been used to map out the excited electronic state manifold. The observations in this recent study are in agreement with the earlier work of others, although the interpretation of previous observations are modified. The manifold of levels proposed is given in Table III. This level scheme is consistent with the original proposal of Orlandi and Siebrand for the decay of the trans form although a higher lying excited state is predicted to cross with the B state. This scheme also explains the nature of the transitions observed in the transient absorption spectra of stilbene and predicts an excited-state absorption in the near-infrared, ~10 000 cm^{-1}. Recently, Abrash et al.[56] have reported a strong absorption in the near-infrared which is consistent with this prediction.

Ground and excited state resonance Raman spectra of the stilbenes, trans[27,28,57,58] and cis,[59] have been used to probe the excited state. For *trans*-stilbene it is found that vibrational relaxation in the S_1 state is rapid, <20 ps, which is in agreement with earlier transient-absorption measurements.[53] The use of optical depletion methods with pulse widths in excess of 40 ps do reveal line broadening of the spectra from "hot" stilbene. The time resolution of this method is estimated to be 10 ps.[27] Gustafson and co-workers[28] have noted the asymmetry in the 1242 and 1567 cm^{-1} bands in the excited-state spectrum which they suggest might indicate the presence of different conformers with differing amounts of phenyl torsion. This hypothesis is consistent with the analysis of the ground state resonance Raman spectra by Myers et al.[58] For the case of *cis*-stilbene the resonance Raman spectrum is particularly enlightening.[59]

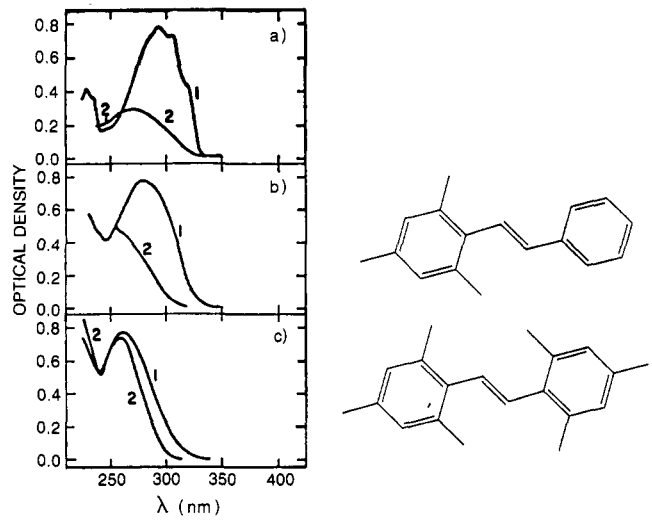

Figure 6. Absorption spectra of stilbene (a), 2,4,6-trimethylstilbene (b), and 2,2',4,4',6,6'-hexamethylstilbene (c) are given for both cis (2) and trans (1) isomers. This figure is taken from ref 68. Copyright 1968 American Chemical Society.

The spectral features indicate a large and rapid vibrational displacement. The initial steps in the photoisomerization are occurring on the femtosecond time scale (25° torsion around the double bond in 20 fs). This rapid motion is consistent with the notion of no barrier for isomerization on the cis side. Much of this difference between the trans and cis is probably caused by the steric hindrance in the cis isomer and the consequent large amount of phenyl torsion.

The effect of substituents on the spectra of stilbenes has been extensively investigated in solutions.[45-47,60-62] Substitution at the para position introduces a red shift which increases with the polarizability/size of the substituent and is approximately additive in going from mono- to disubstituted species.[47] Restricting the discussion to methyl derivatives, it is found that the spectrum of *trans*-stilbene is altered substantially by steric interaction. For *p*-methyl groups the vibrational structure is little changed from that of the stilbene moiety. Although this conclusion is valid in a general sense, it is important to realize that the methyl torsions can couple with the low-frequency modes of the stilbene. Correspondingly substitution in the meta ring positions has little effect on the spectrum, i.e. the distinct conformers have similar spectra. Substitution in the ortho position introduces significant steric hindrance, causing the phenyl rings to twist out of plane (about the ethylene/phenyl bond) and impacts the absorption and fluorescence spectral features. The spectra in Figure 6, parts b and c, are similar to the spectrum of *cis*-stilbene. The phenyl twisting causes the lowest energy electronic transition to undergo a decrease in oscillator strength and a blue shift.

IV. Mechanistics

Superficially the photoisomerization of stilbenes appears quite simple; however, the detailed picture is complicated by the presence of multiple electronic states and multiple intramolecular degrees of freedom. In the simple view, upon electronic excitation the bond order of the ethylene moiety is reduced and twisting about this bond is possible during the excited-state lifetime. The multiplicity (singlet or triplet) of the excited surface upon which photoisomerization occurs is not always clear. In particular, it varies with the nature of the substituents on the phenyl rings. The exact nature of the nuclear motion involved in the isomerization is also at question.

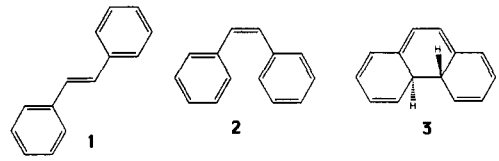

Figure 7. Molecular structures are given for *trans*-stilbene (1), *cis*-stilbene (2), and dihydrophenanthrene (3).

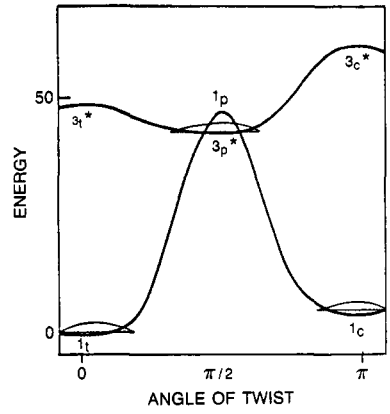

Figure 8. A schematic of the ground singlet and triplet states of stilbene are shown for the twisting coordinate. Reproduced from ref 65b. Copyright 1987 American Chemical Society.

The three major photochemical products formed in stilbene photolysis are shown in Figure 7. The major products in the photolysis of *trans*-stilbene in the near-ultaviolet are *trans*- and *cis*-stilbene. In the case of *cis*-stilbene photolysis the major products are the same, however, DPH can be formed with a quantum yield of 0.10 or more.[63] This pathway is commonly used in the synthesis of phenanthrenes.[64]

A. Trans → Cis

Three mechanisms for the trans to cis isomerization are possible.[1] First, and found to be unimportant, is internal conversion from the first excited singlet state to highly excited vibrational levels of the ground state through which isomerization occurs. Second is through a triplet mechanism which involves an intersystem crossing process followed by isomerization along a triplet surface that either crosses or nearly crosses with the ground singlet surface near 90°.[65] (see Figure 8). This latter mechanism is found to be important in some substituted stilbenes. The third, and commonly accepted mechanism for the isomerization of stilbene, involves twisting about the ethylenic bond in the first excited singlet state to a twisted geometry (presumably 90°) where there is an avoided crossing with the ground state (see Figure 1).

The evidence for this latter mechanism in the isomerization of stilbene rests on a variety of data. Some of the essential observations are given here. First and perhaps foremost are quantum-yield measurements of fluorescence and cis formation with temperature.[66-69] These studies demonstrate that the excited singlet state population is directly correlated with the formation of cis product and that the process is activated. When

these data are combined with triplet sensitization and quenching studies of isomerization, performed by Saltiel and co-workers,[1,65,70] only the singlet mechanism is self-consistent. Second, Sumitami et al.[71] have pumped *trans*-stilbene to the first excited singlet state and monitored the appearance of the cis form. They find that the decay of the trans population matches the rise of the cis formation. This observation is consistent with the singlet mechanism and indicates that the 90° twisted state is very short lived. An upper bound of ~1 ps can be set on this state from the decay characteristics of *cis*-stilbene, assuming the same twisted state is created from both the trans and cis side.[56,72-75] Lastly, Hochstrasser and co-workers[3,36,53] have used transient absorption of the excited singlet to show that vibrational relaxation in the excited state of the trans form is rapid compared to the isomerization rate and that the absorption decay corresponds to the fluorescence decay rate.

B. Cis → Trans

The major relaxation channel for *cis*-stilbene is decay to the ground-state trans and cis forms. The formation of DPH is a minor channel, but may have important implications for the reaction dynamics.[35,76] Early work on the fluorescence spectrum and quantum yield of *cis*-stilbene was performed in glasses or cold solution because of the very rapid nonradiative decay from this state.[41-43] Saltiel et al. have recently recorded the emission spectrum at room temperature in *n*-hexane.[41] The decay of *cis*-stilbene at room temperature has been shown to be less than 2 ps in both the gas phase and in liquid solution.[56,72-75] More recently the fluorescence decay of the excited cis state has been time resolved[73] and the formation rate of the trans ground state from the cis excited state has been time resolved in solution and in clusters.[56,75] The decay kinetics of *cis*-stilbene and the triplet-quenching studies of *cis*-stilbene are consistent with a singlet mechanism. The process is not strongly activated and if there is a barrier along this coordinate it is certainly less than a 1 kcal/mol.

Previous thinking assumed that the formation of the trans isomer occurred only through crossing to the ground-state surface. This view has recently been challenged by Saltiel et al.,[41] who have observed fluorescence emission from the trans isomer after irradiation of the cis isomer.

C. Reaction Coordinate

The use of derivatives to probe the nature of the potential energy surface and the reaction coordinate has been active and fruitful. Two classes of study are (1) the use of steric constraints to probe the nuclear motions involved in the reaction coordinate and (2) the influence of functional group on the electronic character of the potential, singlet vs triplet.

Early studies probed steric effects by substitution of the ethylenic hydrogens with a bulky group and/or substitution of the phenyl rings in the ortho position. Early on it was deduced that substitution of the phenyl rings in the meta and para positions had no recognizable effect on the geometry of the trans form and a small effect on the cis form. When substitutions are made which constrain the phenyl rings from twisting (Φ), the spectral features are similar to that of *trans*-stilbene at

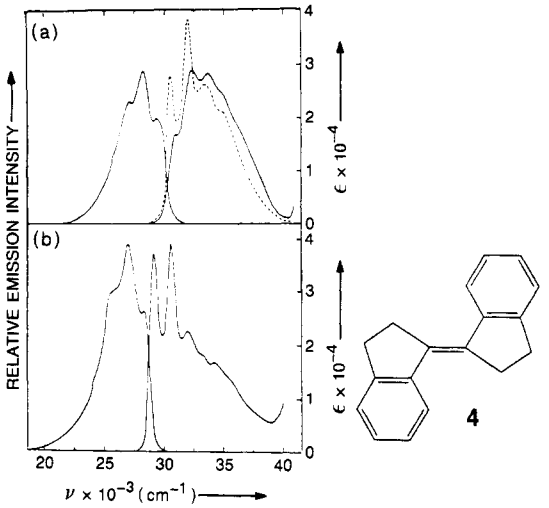

Figure 9. Absorption spectra of *trans*-stilbene (a) and 1,1′-biindanylidene (b) are shown in glycerol at 298 K. The dashed curve in a is taken at 77 K. Reproduced from ref 67. Copyright 1972 American Chemical Society. The molecular structure of 1,1′-biindanylidene (**4**) is also shown.

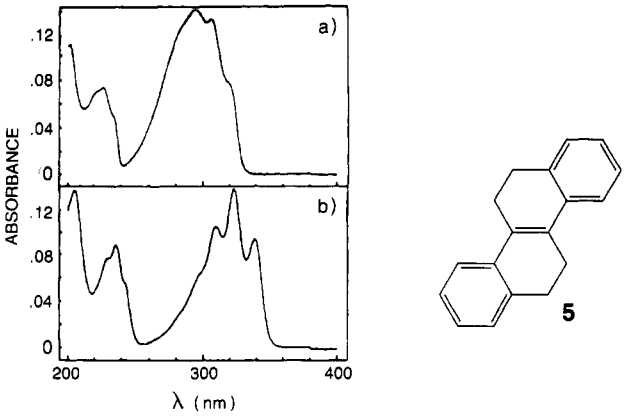

Figure 10. Absorption spectra for *trans*-stilbene (a) and 5,6,11,12-tetrahydrochrysene (**5**) (b) taken at room temperature are shown. Reproduced from ref 78c. Copyright 1986 Elsevier. The molecular structure of **5** is also shown.

very low temperatures in a viscous environment[67] even though the isomerization process is not inhibited by this constraint (see Figure 9). In fact, the isomerization rate increases.[77] If however the rings are tied together so that torsion about the ethylene bond is not possible,[78] the isomerization yield is zero and the fluorescence quantum yield approaches unity. Figure 10 shows the absorption spectra for *trans*-stilbene and the constrained stilbene. These studies show that the primary motion for reaction is ethylenic torsion and that phenyl torsion is less important for the trans isomer. Petek et al.[76] have compared the spectroscopic characteristics of *cis*-stilbene and various analogues. They find similarities between *cis*-stilbene and 1,2-diphenylcyclopentene and suggest that phenyl torsion is of primary importance to the isomerization of *cis*-stilbene.

The study of deuterium-labeled *trans*-stilbene in the isolated molecule and in solution places constraints on the reaction coordinate. Results from these studies[41,49,70,79,80] are summarized in Table IV. When the ethylenic hydrogens are replaced with deuterium, the rate of decay for the trans isomer (d_2) is decreased by ~1.5 times. Replacement of the phenyl hydrogens has little or no effect on the reaction rate. Correspondingly,

TABLE IV. Deuterium Isotope Effect[a]

solvent	T, K	τ_F, ps H_{12}	D_2	D_{10}	D_{12}
hexane	296	82.9	119.7	82.7	123.3
methanol	297	42.6	61.1	44.1	63.1
propanol	294	58.0	76.3	57.3	81.7

[a] Taken from ref 79.

TABLE V. Decay Characteristics of Methylstilbenes in Decane[a] at T = 296 K

solute[b]	number of exponentials	τ_1, ps	% A_1	τ_2, ps
stilbene	1	100	100	
4,4'-DMS	1	309	100	
3,3'-DMS	≥2	105	46	230
3-MS	2	125	93	220
3,3',5-TMS	2	200	50	300
3,3',5,5'-TMS	1	278	100	

[a] Taken from ref 81. [b] 4,4'-Dimethylstilbene (4,4'-DMS); 3,3'-dimethylstilbene (3,3'-DMS); 3-methylstilbene (3-MS); 3,3',5-trimethylstilbene (3,3',5-TMS); 3,3',5,5'-tetramethylstilbene (3,3',5,5'-TMS).

the totally deuterated stilbene has a rate similar to that found for the d_2 case. These studies demonstrate the importance of the ethylenic hydrogens for the reaction of the trans isomer and suggest their involvement in the reaction coordinate (vide infra).

The nature of the reaction coordinate for *trans*-stilbenes has also been probed by studying *m*-methylstilbenes (see Table V). It is apparent from the table that different conformers of the *m*-stilbenes have different isomerization rates. Presumably this change results from a difference in displaced volume upon isomerization and/or from an energetic shift. At room temperature in decane these conformers are distinguishable and the fluorescence decays are nonexponential. As the temperature of the solution is increased, the fluorescence decay becomes more exponential, and as shown by Figure 11 for 3,3'-dimethylstilbene virtually single exponential at 350 K.[33,81] This temperature dependence suggests that phenyl torsion can be competitive with ethylenic torsion. This conclusion is different than that found for binaphthylethylenes[2,82,83] in which the conformer equilibrium is believed to be frozen

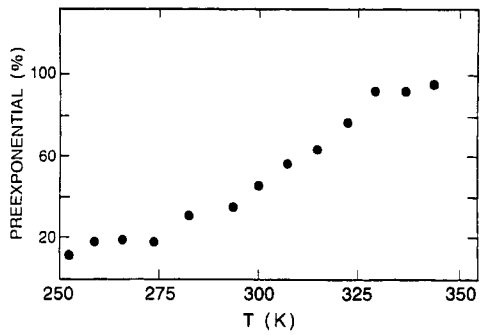

Figure 11. The percentage of short-lifetime component is plotted versus temperature for 3,3'-dimethylstilbene in decane. Reproduced from ref 33. Copyright 1990 Elsevier.

on the excited-state time scale. Alternatively, the different conformers may have different activation barriers to isomerization, but as the temperature increases the isomerization rates of the distinct conformers become similar. A more detailed study should distinguish these two possibilities.

The reaction coordinate for *cis*-stilbene is not very well understood either, but the lack of a barrier and the rapid dynamics may make the motions directly accessible spectroscopically. Recently Abrash et al.[56] have performed polarization studies of the formation of *trans*-stilbene from the cis form and they find that the orientation of the C_2 axis in space is little changed by the reaction. This measurement places important constraints on the nature of the reactive motion. These workers suggest that small amplitude motions of a large number of atoms are involved in the reaction rather than a simple twist. This view also finds support from the resonance Raman studies of *cis*-stilbene.[59]

D. Singlet vs Triplet

The influence of substituents on the state dependence of the isomerization has been studied through directly monitoring the triplet state with transient-absorption methods[84-88] and by triplet-quenching studies of the isomerization yields.[88,89] Most of these studies have involved substitution at the meta (3,3', 5,5') and para (4,4') sites of the phenyl ring. The nature of the substituent can have a profound effect on the excited-state

TABLE VI. Quantum-Yield Data for Various Stilbenes[a]

substituents	triplet yield ϕ_t	ϕ_c	isomerization yields $\phi_{t\to c}$	$\phi_{c\to t}$	fluorescence yield: ϕ_F	solvent	mechanism	refs
none	0.002	-	0.52	0.35	0.035	C_5	S	68, 89
4-Cl	0.48	-	0.60	0.42	0.070	MCH-IH	S and T	68, 87
4-F	0.17	-	0.5	0.4	0.04	MCH-IH	S	68, 87
4-Br	0.33	-	0.52	0.35	0.044	C_5	S and T	68, 87, 89
3-Br	0.17	-	0.56	0.34	0.014	C_5	S and T	89
3-Br, 3'-Br	0.34	-	0.56	0.24	0.019	C_5	S and T	89
4-NO_2	0.86	0.59	0.50	0.34	<IE-4	Bz	T	84
4,4'-NO_2	0.81	0.55	0.47	0.30	<IE-4	Bz	T	84
4-NO_2, 4'-MeO	0.93	0.27	0.53	0.37	0.006	Bz	-	84, 90
4-NO_2, 4'-NH_2	-	-	0.45	-	0.002	MCH	S and T	86
4-NO_2, 4'-DMA	-	-	0.28	0.4	0.30	MCH	S and T	86, 88
4-NO_2, 4'-DEA	-	-	0.20	-	0.36	MCH	S and T	86
4-CN, 4'-DMA	-	-	0.45	-	0.03	Tol		85
4-CN	-	-	0.42	0.45	-	Bz	S	85
4-CN, 4'-CN	-	-	0.45	0.35	-	C_5	S	85
4-CN, 4'-MeO	-	-	0.40	0.40	0.013	Bz or Tol	S	85, 90

[a] Bz, benzene; C_5, pentane; Tol, toluene; T, triplet; S, singlet; MCH-IH, methylcyclohexane-isohexane; ϕ_F, fluorescence yield; DMA, dimethylamino; DEA, diethylamino.

mechanism. The results of this work are summarized in Table VI for some selected species. More complete tabulations of this work are available.[1] It is found that the singlet and triplet mechanisms are always present. When the functional group increases the coupling between the singlet and triplet manifolds, the triplet mechanism becomes more competitive. In the case of nitro-group substitution the triplet mechanism dominates the singlet route, whereas in the alkyl substituent case the singlet mechanism is dominant. In the case of bromostilbene[88,89] the isomerization appears to proceed by a combination of the two processes. In general it is found that the intersystem-crossing process is not strongly activated whereas the singlet process is activated. The differing temperature dependence and the presence of both mechanisms can effect the interpretation of dynamical studies.

Asymmetrically substituted stilbenes can display even more varied behavior.[90-96] When one end of the molecule is a good electron-donor group and the opposite end is a good electron-accepting group, intramolecular charge transfer is possible. Numerous reports of twisted intramolecular charge transfer (TICT) states have appeared recently. The excited state forms a large dipole moment (in excess of 20 D)[95,96] and the relaxation dynamics depends strongly on solvent polarity. This charge-transfer state can provide another relaxation pathway which competes with the two isomerization pathways.

E. Solvent Effects

Three general types of solvent effects have been observed for the isomerization of stilbenes. Best known is the slowing of the reaction rate with increase of the solvent friction, or viscosity. This effect is discussed in detail below and is characteristically a dynamical effect. Second is the sensitivity of the rate to the polarity of the solvent which results from the dipolar character of asymmetrically substituted stilbenes and the polarizable character of the *trans*-stilbene transition state. The polarity can effect both the dynamics and the pathway of the reaction (vide infra). Last is the influence of "heavy" solvents on the reaction pathway via the external heavy-atom effect. The influence of solvent on the intersystem-crossing rate in stilbenes can be significant for solvents containing heavy halogen atoms and has been discussed by Saltiel.[1]

V. Theoretical Considerations

The theory of reaction dynamics in the condensed phase is receiving considerable attention. Much of the recent progress has been reviewed.[97-101] Explicit treatments of the isomerization of stilbene[102] have been performed. Most of the models treat the case of an adiabatic barrier crossing in a fluid; however, some work on nonadiabatic isomerization is available.[103] The discussion here will address the models commonly used in comparison with rate data.

A. Statistical Models

1. Isolated Molecule

Unimolecular reactions in the gas phase have been successfully described with statistical models for the distribution of activated molecules.[104,105] The transition-state theory (absolute-rate theory or activated-complex theory) assumes an equilibrium between the reactant and the activated complex. The expression obtained for the rate constant is

$$k_{TST} = \langle \kappa \nu \rangle \frac{Q^{\ddagger}}{Q_r} \exp(-\beta E_0) \tag{1}$$

where $Q^{\ddagger}$ is the canonical partition function of the activated complex, Q_r is the canonical partition function of the reactants, β is $(kT)^{-1}$, and E_0 is the difference in zero-point energy between the activated complex and the reactants. The frequency factor ν represents the frequency of reactants crossing the transition-state region and the transmission coefficient κ accounts for recrossings of this region. This product appears as an average over all $6N$ dimensions of the activated complex. This equation is usually simplified by replacing the full partition function of the activated complex with a partition function that has the contribution from the reaction coordinate, q^*, extracted and assuming a flat barrier so that $q^* \rightarrow kT/h\nu$. In this limit and assuming $\kappa = 1$, one obtains

$$k_{TST} = \frac{kTQ^{\ddagger}}{hq^*Q_r} \exp(-\beta E_0) \tag{2}$$

which can be written in thermodynamic form as

$$k_{TST} = \left(\frac{kT}{hq^*}\right) \exp\left(\frac{\Delta S^{\ddagger}}{R}\right) \exp\left(\frac{-\Delta H^{\ddagger}}{RT}\right) \tag{3}$$

A further approximation concerning the width, δ, of the transition-state region (namely $\delta = \Lambda$, where Λ is the deBroglie wavelength) leads to $q^* = 1$.

For the case of a microcanonical ensemble the formulation of the rate expression is given by RRKM theory through similar assumptions. By performing a thermal average of the RRKM rate, the transition-state theory (TST) result given here can be recovered. The RRKM rate constant, $k(E)$, is given by

$$k(E) = \frac{W(E - E_0)}{h\rho(E)} \tag{4}$$

where $W(E - E_0)$ is the number of activated states and $\rho(E)$ is the density of states.

2. Solvated Molecules

At low gas densities the reaction rate increases with an increase in collision frequency because collisions provide the energy needed to attain the threshold energy. As the collision frequency becomes very high, however, the collisions (or friction) impede the reaction and the rate decreases. This turnover of the rate's dependence on friction is referred to as the Kramers turnover and has been observed for multiple reactions,[106,107] including that of stilbene.[108-110] Figure 12 shows a sketch of the expected rate behavior with friction.

The most widely used model for the description of isomerization dynamics is that of Kramers[111] who treats the reactive motion as the escape of a particle over a potential barrier in one dimension. The model potential is sketched in Figure 13. The particle is initially bound in the potential well on the left at A, must pass over the

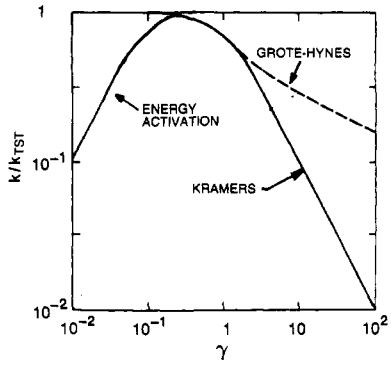

Figure 12. A log–log plot of the isomerization rate versus the static friction constant is given. The solid line shows the energy activation region at low friction, the Kramers turnover, and the diffusive limit at high friction. The dashed line shows the effect of non-Markovian friction as discussed by Grote and Hynes. Adapted from ref 99. Copyright 1988 American Chemical Society.

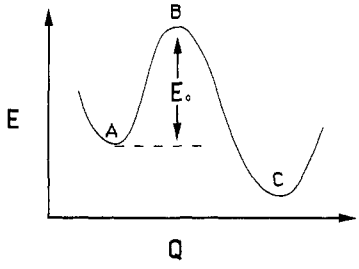

Figure 13. A schematic of the potential energy diagram used in the Kramers model is shown.

barrier of height E_0 at B to arrive at the product C on the right. The coordinate Q in our case is the isomerization coordinate, i.e. an angle. Kramers writes the Langevin equation to describe the dynamics of the particle

$$\dot{p} = -\zeta p + F(t) + K(Q,t) \tag{5}$$

where $\dot{p}$ is the time derivative of the particles momentum and $K(Q,t)$ is the force on the particle from the potential. The terms arising from the bath are a dynamical friction ($-\zeta p$) and a stochastic force ($F(t)$) with zero average which is characteristic of Brownian motion. The solution to this equation is used to calculate the flux of population across the barrier, the rate of reaction.

The Langevin equation is a stochastic differential equation and its solution must involve the probability distribution of the position, Q, and/or that of the velocity, u. The solution can be simplified by assuming a separation of time scales. Kramers assumes that there is a time, τ, which is so short that the velocity changes little but is so long that the value of $F(t + \tau)$ is independent of $F(t)$. This assumption is that of a Markovian process whose probability distribution W ($\equiv W(Q,u,t)$) depends only on its value at a previous time $t - \tau$. This assumption allows Kramers to use the Fokker–Planck equation, which describes the time evolution of probability density for the Brownian particle in phase space. The Fokker–Planck equation is

$$\frac{\partial W}{\partial t} + u\frac{\partial W}{\partial Q} + K\frac{\partial W}{\partial u} = \zeta u\frac{\partial W}{\partial u} + \zeta W + \frac{\zeta kT\partial^2 W}{m\partial u^2} \tag{6}$$

where the left side is the Stokes operator and the right side is the stochastic element.[112] Kramers solved this equation with the following assumptions: (a) if at initial time the particles are in A and $E_0 \gg kT$, then a quasi-stationary state exists (i.e., $\partial W/\partial t = 0$), (b) the potential near A and B can be described by a harmonic oscillator potential (with ω_0 for the frequency at A and ω' for the frequency at B), (c) a Boltzmann distribution of velocities exists near A, (d) at some point past the top of the barrier, passage to product is certain (i.e. no appreciable backreaction).

He obtains the expression

$$k_{iso} = k_{TST}[(1 + (2\omega'\tau_v)^2)^{1/2} - 1]/(2\omega'\tau_v) \tag{7}$$

where τ_v is the velocity relaxation time and is related to the friction coefficient ζ by $\tau_v = \mu/\zeta$ (μ is the effective mass of the particle). The rate constant k_{TST} is given by eq 1 and excludes frictional effects.[97] This expression is commonly written as

$$k_{iso} = F(\zeta)\exp(-E_0/RT) \tag{8}$$

It is useful to consider two natural limits of expression 7. In the first limit, the velocity relaxation time τ_v is very long compared to "free motion" time scales, i.e. the frictional forces are a small perturbation on the free motion. In this regime the isomerization ought to be proportional to the friction[111-117] because the collisions with the solvent cause the distribution function to sample the range of available energies. Alternatively, collisions provide energy for escape over the barrier instead of oscillatory motion in the potential well. In this respect, expression 7 is incorrect since it becomes independent of ζ in this limit. This feature has been considered by Kramers and corresponds to the energy-controlled regime which he discusses. The second limit is that of very large friction. In this case, τ_v is short compared with the characteristic time scale of free motion on the potential surface. In this "Smoluchowski limit" eq 7 is shown by expansion in $\omega'\tau_v$ to yield

$$k_{iso} = (\omega_0\omega'\tau_v/2\pi)\exp(-E_0/RT) \tag{9}$$

and the rate is inversely proportional to the friction.

The Kramers view can be generalized through the use of the generalized Langevin equation (GLE)

$$\dot{p}(t) = K(Q,t) - \int_0^t d\tau\zeta(\tau)p(t-\tau) + F(t) \tag{10}$$

and

$$\zeta(t) = (\beta/\mu)\langle FF(t)\rangle \tag{11}$$

In this expression, the friction is time (or frequency) dependent and is related to the autocorrelation function of the stochastic force as given by eq 11. This equation allows for correlations in the random force term and relates these correlations to the friction. Considerable efforts have been made in this vein,[97-99,118] most notably the work of Hynes and co-workers.[119] These workers solve this equation for the barrier crossing problem and find the rate constant to be

$$k = k_{TST}(\lambda/\omega') \tag{12}$$

where

$$\lambda = \omega'^2/[\lambda + \zeta(\lambda)] \tag{13}$$

Hynes refers to λ as the reactive frequency. It is related to the transmission coefficient by $\kappa = (\lambda/\omega')$ and is determined by the self-consistency relation (eq 13). The

frequency-dependent friction is determined at the reactive frequency and is defined by

$$\zeta(\lambda) = \int_0^\infty dt\zeta(t)\exp(-\lambda t) \quad (14)$$

Rearrangement of the rate expression gives

$$k = k_{TST}[(1 + (\zeta(\lambda)/2\omega')^2)^{1/2} - (\zeta(\lambda)/2\omega')] \quad (15)$$

which is the Kramers expression with the friction replaced by the frequency-dependent friction. In the limit that the force fluctuations are δ correlated the frequency-dependent friction is given by $\zeta(\lambda) = \zeta$, and the Kramers result (eq 7) is recovered.

B. Friction

Comparisons of the measured rate data with these models has been possible, but is hampered by the modeling of the friction. Various approaches have been used. By far the simplest (perhaps crudest) approach assumes that the friction is proportional to the zero-frequency solvent shear viscosity [Debye–Stokes–Einstein (DSE) relation], $\zeta \propto \eta$, which results in

$$F(\zeta) = A_1[(1 + (\eta/A_2)^2)^{1/2} - \eta/A_2] \quad (16)$$

where $A_1 = \omega_0/2\pi$ and $A_2/\eta = 2\omega'\tau_v$. With this method significant deviations are found between experiment and theory. A better modeling (i.e. better in the sense of more microscopic) of the friction in terms of a solvent parameter can be obtained by using the light-scattering relaxation time, τ_{ls}, of the solvent.[120,121] Alternatively, one can estimate the collision frequency in the fluid and use that as a measure of the friction. One method to estimate this parameter for liquids is by the relation

$$\tau_{col}^{-1} = \rho d^2/6\eta \quad (17)$$

where d is the solvent molecule diameter and ρ is the solvent density.[122] These different methods use a solvent/solvent friction measure and assume it is proportional to the solute/solvent friction.

Robinson and co-workers[123,124] have proposed using the shear viscosity of the fluid to measure the friction but not as given by the DSE form. They propose using

$$\zeta = \frac{A_0\omega' I_r}{F(\zeta)}\left(\frac{\eta}{a + b\eta}\right) \quad (18)$$

where A_0, a, and b are adjustable parameters and I_r is the reduced moment of inertia. This form results in a friction which is proportional to the viscosity when the viscosity is small and is independent of the viscosity when it becomes large. This expression also includes a frequency dependence by its inverse dependence on the reduced isomerization rate, $F(\zeta)$. This form of the friction is able to fit both experimental data and molecular dynamics simulation results quite well. Analysis of the molecular dynamics simulations indicates that this form models the contributions of a solvent inner sphere (η independent) and a solvent outer sphere (η dependent) to the friction.

A microscopic measure of the solute/solvent friction can be found by measuring the diffusion coefficient of the isomerizing moiety, or of the whole stilbene, in the solvent of interest. This procedure was first proposed by Velsko et al.[125] in a study of the isomerization of the dye molecule DODCI. This approach has been used with both translational (D_T)[126,127] and rotational (D_{or})[77,125,127,128] diffusion coefficients and has obtained a moderate amount of success (vide infra). This empirical measure probes the solute/solvent friction on time and space scales more appropriate to the isomerizing moiety. Hochstrasser and co-workers[77,128] carry this approach one step further via the Hubbard relation

$$\tau_\omega = I/(6kT\tau_{or}) \quad (19)$$

where τ_{or} is the rotational relaxation time of the solute ($\tau_{or} \propto D_{or}^{-1}$). In the limits of small step diffusion and exponential relaxation of the angular velocity correlation function, τ_ω corresponds to the angular velocity relaxation time. This measure of the friction is somewhat closer to a collision frequency and corresponds to the velocity relaxation time discussed by Kramers.

The Grote–Hynes result suggests the importance of using a frequency-dependent friction. Many models for the frequency-dependent friction are possible. Bagchi and Oxtoby[129] showed that a hydrodynamic model for the frequency-dependent viscosity of a solvent and the DSE relation for the friction could be used to model the data. Jonas and co-workers[130] have found it useful to model the force correlation function as a damped sinusoid and vary the parameters of this functional form to fit data. These approaches include the frequency-dependent response of the solvent's contribution to the friction. The form of the friction found by Grote and Hynes includes contributions from both the solvent and other nonreactive modes of the solute. The other degrees of freedom of the solute can also be treated by a multidimensional picture.

C. Multidimensional View

Generalizations of the stochastic description of reaction rates to many dimensions has been undertaken.[131–135] One effect of dimensionality is the presence of coupling of the reactive mode to other nonreactive modes in the molecule which can act as a channel to the thermal bath of nonreactive degrees of freedom. This coupling represents an internal friction in the molecule and can either increase or decrease the reaction rate, depending on whether one is in the high- or low-friction limits.[98,116] Another effect of dimensionality can result from anisotropy in the friction. With the reaction occurring on a multidimensional energy surface, motion along one coordinate could have a stronger coupling to solvent friction than motion along some other coordinate. It is possible in this case for the reaction coordinate to change as the friction changes.[132,136] This process will also be strongly influenced by anisotropy in the potential energy surface, and the interplay between these two effects can be complicated.

D. Polarity

The effects of solvent polarity are important for stilbenes and models of reaction rates under the conditions of both equilibrium and nonequilibrium solvation are becoming available.[133,137–140] Two primary methods are useful for addressing the role of solvation. One is to consider the reaction as occurring along an "equilibrium solvated" reaction coordinate and incorporate nonequilibrium solvation effects into a fre-

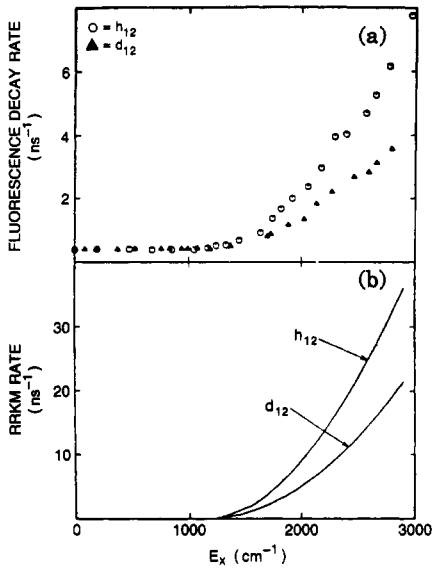

Figure 14. The fluorescence decay rate of *trans*-stilbene (H_{12}) and *trans*-perdeuterostilbene (D_{12}) as a function of excess vibrational energy in the first excited singlet state (a). The bottom figure (b) shows the prediction of a "standard" RRKM calculation and differs in magnitude from the experimental data by a factor of 5 or more. Reproduced from ref 142b. Copyright 1985 American Chemical Society.

quency-dependent friction.[137] Alternatively, one can use a multidimensional model which includes a solvent coordinate (or polarization coordinate) explicitly.[133] Both of these approaches have been found to accurately represent the experimental observations, at least qualitatively.[141]

VI. Reaction Dynamics

A. Isolated Molecule Rates

1. trans-Stilbene

Numerous groups[36,79,142-144] have studied the isomerization rate of stilbene under isolated molecule conditions, both in a jet expansion and in a thermal ensemble. The excess energy dependence in a jet-cooled sample shows a threshold behavior (see Figure 14). The decay rate at zero excess energy is in excellent agreement with the expected radiative lifetime of stilbene. As the excess energy increases the population decay rate of the trans state is constant until a threshold near 1200 cm^{-1} at which it begins to rise. The decrease in isomerization rate with deuteration of the molecule is in qualitative accord with the prediction of RRKM theory. As shown in Figure 14, parts a and b, the difference in magnitude of the observed decay rates and the theoretical prediction is large.

The complexity of the stilbene spectrum suggests that intramolecular modes may be strongly coupled. Felker et al.[145] have probed the extent of intramolecular vibrational redistribution (IVR) in the regime between zero and an excess energy of 1332 cm^{-1}. In the excess-energy regime below 752 cm^{-1} they find that IVR is absent on the time scale of fluorescence (2.6 ns). The intermediate energy regime from 789 to 1179 cm^{-1} corresponds to restricted IVR and vibrational coherence effects are observed. At energies in excess of 1230 cm^{-1} IVR is dissipative and the fluorescence decays have time constants of tens of picoseconds. The onset of dissipative IVR corresponds well to the threshold for isomerization, and may reflect a connection between these two processes. Attempts have been made toward understanding rotation–vibration and vibration–vibration coupling in a thermalized ensemble by two groups.[146-148] The results of these studies are consistent with the view of rapid vibrational relaxation in the isolated molecule. Whether IVR is complete on the time scale of reaction remains at question.

RRKM theory has been applied to the isomerization rates for both the jet studies, $k(E)$, and the bulb studies, $k(E,T)$. The energy dependence of the isomerization rate can be brought into quantitative agreement with RRKM predictions. Zewail and co-workers[142,145] found that if one uses a threshold energy of 1200 cm^{-1}, chooses a reactive mode frequency of 400 cm^{-1}, and assumes that all other vibrational modes do not change in frequency on going from the reactant to the transition state, RRKM theory predicts rates too large compared to those observed in the jet (see Figure 14). Similar observations were made by other groups.[79,149-151] Zewail and co-workers[142,145] discuss a variety of mechanisms for this discrepancy, including restricted IVR, reversible reaction, multidimensional effects, and nonadiabatic effects. Using a nonadiabaticity factor for crossing at the transition state with a higher lying state brought RRKM predictions into agreement with the observed rates. As a self-consistency check these authors found that the energy dependence for the decay rate of perdeuteriostilbene was in good agreement with this modified RRKM model when one used the same nonadiabaticity parameter for stilbene (H_{12}) and perdeuteriostilbene (D_{12}). More recently Troe and coworkers[106,109,143] point out that good agreement between the modified RRKM model and the observed rate constant, $k(E)$, is not unique because of the number of adjustable parameters one can vary for a good fit. They choose to represent the $k(E)$ data by a modification of the threshold energy (an increase to 1300 cm^{-1}), different choice of reaction coordinate (88 cm^{-1}), and scaling of reactive and transition-state frequencies. They discuss the utility of this "optimized" RRKM approach for comparison with data in solution. Rademann et al.[149] have further tested the RRKM picture by alkyl substitution in the para position of the phenyl moiety (4-methylstilbene, 4-ethylstilbene, and 4-propylstilbene). They find the counterintuitive result that the isomerization rate increases as the number of bath modes in the molecule increases. They interpret this effect as a lowering of the threshold energy with an increase in the size of the alkyl substituent (ca. 100 cm^{-1} per CH_2).

For the case of a thermal distribution of excited states, nonexponential fluorescence decays are observed, whereas the fluorescence decays at a well-defined energy are exponential. Fleming and co-workers[4,150,151] have shown that the convolution of the thermal ensemble of vibrational and rotational states with the $k(E)$ rates from the jet reproduce the observed fluorescence decays quite well. The nonexponentiality results because "hot" molecules (energy in excess of the threshold for isomerization) react rapidly, and in the isolated molecule case the colder molecules (excess energy below the threshold energy) must decay radiatively. This view is also supported by the observation that as the buffer gas

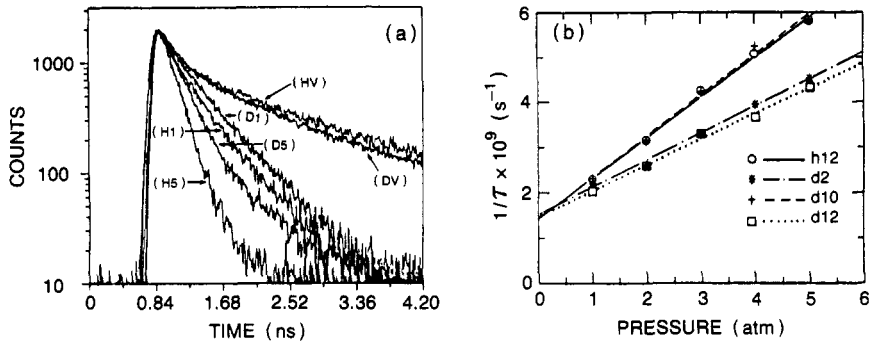

Figure 15. (a) Observed decay curves for stilbene (H_{12}) and perdeuterostilbene (D_{12}) are shown at T = 296 K. (HV = stilbene vapor; DV = stilbene-d_{12} vapor; H1 = stilbene in 1 atm methane; D1 = stilbene-d_{12} in 1 atm methane; H5 = stilbene in 5 atm methane and D5 = stilbene-d_{12} in 5 atm methane). (b) Decay rates of the four deuterated stilbenes are plotted versus methane gas pressure. The rates are weighted averages from the double exponential fits. Reproduced from ref 79. Copyright 1988 American Chemical Society.

pressure rises and collisions occur on the excited-state time scale, the decays become more exponential. The collisions with buffer gas molecules keep the ensemble of stilbene at a fixed temperature. As with the isolated molecule, the magnitude of the rates are much larger than that predicted by a simple RRKM treatment. These workers suggest that the increase in rate over that expected from a simple RRKM model probably results from a breakdown in the energy randomization assumption for stilbene.

More recently, Courtney et al.[79] have probed the pertinence of the RRKM model through a set of isotopic labeling studies of *trans*-stilbene and measurement of the decay rates in jet expansion and under bulb conditions. The observations for the rate are shown in Figure 15. The trend in the rates is such that deuteration of the ethylene hydrogens provides similar rates (i.e. D_2 and D_{12}) which are distinctly lower than that of the perhydro compound, whereas deuteration of only the phenyl hydrogens (D_{10}) provides rates similar to that of the perhydro compound (H_{12}). Although a simple RRKM treatment can be adjusted to fit the data for any two of these four solutes, it does not predict the trend in the solute series. Variation of the threshold energies can be used to explain the trend in the data, but large changes in this quantity would be inconsistent with the Arrhenius plots for the thermal data (where the activation energies are indistinguishable). These workers suggest that incomplete IVR could explain the data. Recently Nordholm[80] has used a model for restricted IVR that reproduces the trend observed by Courtney et al. Nordholm is able to reproduce the trend in the $k(E)$ and $k(T)$ data for the four isotopomers by assuming that the barrier increases by $\sim$150 cm^{-1} when the ethylenic protons are deuterated. This effect can be generated by choosing a "hydrogenic bridge mode" for the reaction coordinate or allowing these modes to have much lower frequencies (factor of $\sim$2) in the activated complex. Most recently Negri and Orlandi[176] have reproduced the trend in rates upon deuteration by using a nonadiabatic scheme similar to that proposed by Zewail and co-workers.[142,145] These values use the QCFF-PI method to obtain the structural features of the transition state and use these properties to compute the RRKM rate constants.

2. *cis*-Stilbene

Yoshihara and co-workers[40,75,76] have been investigating the spectroscopy and kinetics of *cis*-stilbene under supersonic jet conditions. Laser-induced fluorescence spectra from van der Waals clusters of *cis*-stilbene and rare gas atoms indicate a shallow well in the excited state. The isomerization rate of *cis*-stilbene under jet conditions appears to be rapid and multiexponential, a few picoseconds. These rates are determined from the appearance of the trans isomer, demonstrating that the rapid decay of the cis form yields considerable trans isomer and that any delay in crossing to the ground-state surface is short. This latter observation agrees with conclusions from bulb experiments.[74] More recently these workers have studied the spectral and fluorescence lifetime properties of a series of *cis*-stilbene analogues, both rigid and nonrigid. Comparisons between the different compounds suggest that the initial stages of the cis to trans isomerization [phenyl torsion] is along a reaction coordinate appropriate for the formation of DPH. These workers propose that steric repulsion between the phenyl rings causes significant C_e–phenyl twist which couples with ethylenic torsion leading to isomerization.

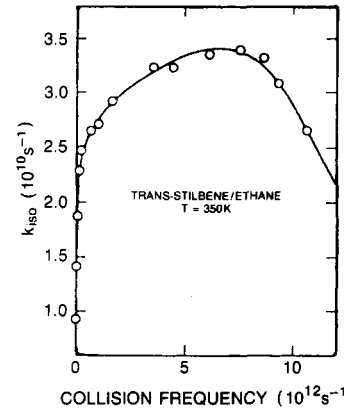

Figure 16. The isomerization rate of *trans*-stilbene as a function of collision frequency is shown at 350 K in ethane. Reproduced from ref 110. Copyright 1985 Elsevier.

B. Low-Friction Regime

This regime corresponds to stilbene isomerization in a dense buffer gas, where collisions are rapid enough to maintain a thermalized distribution of stilbene molecules but slow enough that the barrier crossing is in the energy-controlled limit. The expectation is that the isomerization rate in this limit will increase as the friction, or collision frequency, increases (as in Figure 15b). This regime was first identified by three groups

almost simultaneously.[108-110] Figure 16 shows this regime for *trans*-stilbene in ethane at pressures below 120 atm by Hochstrasser and co-workers.[110] The data show the rise, plateau, and decline of the rate with increasing friction, in qualitative accord with Kramers' prediction. The plateau region is quite broad. All three reports show a clear increase in the rate with an increase in collision frequency in dense gas.[108-110] The data can be fit throughout the turnover region by the use of the connection formula

$$1/k = 1/k_0 + 1/k_\infty + 1/k_{diff} \qquad (20)$$

where k_∞ is the limiting rate constant at high gas pressure, k_0 is the low-pressure rate constant, and k_{diff} is the rate constant in the diffusive limit.[109] This ad hoc relationship interpolates the rate constant through friction regimes in which the dynamics changes dramatically. This formula is analogous to treating the processes serially so that the slowest one dominates the rate. Recently Schroeder et al.[109] have reported a study of the isomerization of stilbene over a wide friction range in each of seven different solvents. They find that eq 20 accurately represents the friction dependence in a single solvent with a barrier ~1.5–2 kcal/mol. The turnover region of the isomerization rate shifts along the friction axis with a change in the solvent. They attribute this shift to a modification of the potential energy curve via solvation from cluster formation.

A puzzling and controversial feature of the isomerization rate of stilbene is the order of magnitude or greater *increase* of the rate for the solvated molecules over that of the isolated molecule, even when the isolated molecule is energized above the threshold energy. The explanation for this behavior may very well be linked to the dynamics effecting the comparisons with RRKM theory for the isolated molecule. Zewail and others[142,176] have suggested that when the stilbene is surrounded by solvent the nonadiabaticity of the reaction is reduced (because more time is spent near the curve crossing), leading to higher rates. In contrast Troe has proposed that solvation lowers the energy barrier to reaction and that at low densities solvated clusters of stilbene with the buffer gas are formed.[109,152] Other workers[153,154] have reported barriers in solution similar to those found in the jet, which would appear to invalidate this latter proposal. It may be that the barrier effects in liquids are strongly linked to other processes, such as viscous dissipation. Saltiel and coworkers[155] have proposed a method for separating solvation effects on the barrier from viscosity effects and conclude that the intrinsic barrier is close to the isolated molecule value. The solvents studied by Troe are all physically smaller than stilbene and may solvate the molecule better than do the alkane solvents used for the liquid-phase studies, although such a result would be surprising. Lastly it should be noted that restricted IVR could account for the reduced rates in the gas phase.[79,80]

C. Intermediate- to High-Friction Regime

The onset of the Kramers turnover in *trans*-stilbene occurs at viscosities of 0.015–0.035 cP (collision frequencies of 3–9 ps^{-1}) in ethane and at similar values in other solvents. The intermediate- to high-friction regime corresponds to viscosities in excess of these values, ranging from the dense gas to liquids and solids. Many groups have probed the isomerization of stilbene and its simple analogues in this regime. The discussion here will be divided into two parts, studies in nonpolar solvents[55,69,77,108,128,153-161] and studies in polar solvents.[120,141,162-165] This subdivision is made because solvation effects on the reaction dynamics in nonpolar solvents, if present, tend to be small and rapid. In polar solvents, especially alcohols, the solvation effects can be large and slow, which necessitates a more explicit treatment of the solvent dynamics. From a more general perspective, the Kramers model and simple friction ideas go far in explaining the data and provide a framework for understanding condensed-phase chemical reactions.

1. Nonpolar Solvents

a. Identifying a Barrier. In order to compare the measured rates with statistical models it is useful to isolate the dynamical factor, $F(\zeta)$, in the rate expression. This factor, given by eqs 7 and 8 in the Kramers model, will be referred to as the reduced isomerization rate. Different methods have been used to separate the energy barrier effect from the reduced isomerization rate. All of these methods assume that the energy and friction effects can be separated. In the case of *trans*-stilbene the energy threshold is known for the isolated molecule (3.2–3.8 kcal/mol).[142-144]

The clearest method is to measure the isomerization rate of the molecule in a single solvent as a function of temperature and pressure.[106,109] By keeping the collision frequency or viscosity constant (through control of pressure) and varying the temperature an activation curve can be obtained for the reaction. By assuming that the activation energy corresponds to the energy barrier to reaction, the reduced isomerization rate can be extracted from the measured rate data. This method assumes that the energy barrier is not a strong function of the pressure. A self-consistency test for this method is to perform activation plots over different pressure and temperature ranges.

A second method is to measure the isomerization rate in a homologous solvent series (e.g., *n*-alkanes) which minimizes variations from the differences in solvation of different solvents. By adjusting the temperature in each solvent, Arrhenius plots can be constructed for the rate in which the solvent friction (measured by viscosity, collision frequency, or some other parameter) is kept constant while the temperature and member of the homologous series are varied. These Arrhenius plots are referred to as isoviscosity or isofriction plots. This procedure assumes that solvation effects throughout the series are small and that the form of the solvent friction does not depend on the member of the solvent series. Two self-consistency checks for this method are that the Arrhenius plots have the same slope when performed at different viscosities and that different measures of the friction (e.g. viscosity and collision frequency) provide the same slope.

Saltiel and co-workers have proposed an alternative approach for identifying the activation energy, or enthalpy, from viscosity effects.[67,155] This approach exploits the form of eq 3. A plot of $\ln (k_{iso}/T)$ vs $1/T$ in any given liquid solvent gives a slope which corresponds to the activation enthalpy. The enthalpy which results

TABLE VII. Isoviscosity Parameters for Alkylstilbenes in Alkanes[a]

	trans-stilbene		4,4'-DMS[c]		4,4'-TBS[c]	
viscosity, cP	E^b	solvents	E^b	solvents	E^b	solvents
0.3					4.26	C_6–C_8
0.4	3.5	C_2, C_3	4.02	C_6–C_{10}	4.60	C_8–C_{10}
0.6	3.4	C_2, C_3	4.23	C_7–C_{12}	4.73	C_{10}–C_{13}
0.8			4.26	C_8–C_{14}	5.06	C_{12}–C_{14}
1.0			4.48	C_9–C_{16}	5.17	C_{13}, C_{14}, C_{16}
1.2	4.5	C_{10}–C_{16}				
1.6	4.0	C_{10}, C_{12}, C_{14}	4.53	C_{11}–C_{16}		
2.0	4.0	C_{10}, C_{12}, C_{14}	4.62	C_{12}–C_{16}		
2.4			4.65	C_{13}–C_{16}		

[a] Taken from refs 108, 153, 154, 167. [b] E is in kcal/mol. [c] 4,4'-DMS is 4,4'-dimethylstilbene and 4,4'-TBS is 4,4'-di-*tert*-butylstilbene; C_n represents a normal alkane with n carbon atoms.

is associated with an intrinsic barrier and a solvent-induced barrier (via the viscosity). The solvents contribution does not correspond to the full activation energy of the solvents' viscosity, but a fraction thereof. The fraction is determined by requiring all the solvents (in the stilbene case alkanes and glycerol) to contribute the same fraction of their respective viscosity activation energies. This result is quite successful at correlating the data and is related to the power-law form of the viscosity dependence used by other workers.[68,108,120,141,153,154] The power-law form for the rate constant is

$$k_{iso} = (B/\eta^a) \exp(-E_{act}/RT) \qquad (21)$$

where B and a are adjustable parameters and E_{act} is either obtained from one of the first two methods or treated as a parameter (the last method). A wide range of systems in a wide range of solvents can be fit to this functional form quite well. Unfortunately the origin of this form from theoretical considerations in unclear. A free-volume model of the fluid can be used to interpret these parameters, but is found to be inconsistent when different-sized solutes are compared.[120,154] This inconsistency can be resolved by using a microviscosity in eq 21.[126,166] Because of the good fits obtained with this model, the parameters of eq 21 can be used to compare different solutes and solvents.

For *trans*-stilbene in the *n*-alkanes these methods provide somewhat different values for the activation energy. In the high-pressure studies of Troe[109] in ethane, propane, and butane energy barriers of 1.8 kcal/mol are obtained from temperature studies at constant friction through the variation of pressure. This value stands in contrast to the higher barriers obtained from the threshold energy for the isolated molecule. Troe and co-workers have attributed this drop in energy barrier to solvation of the stilbene by the alkane solvent. Isoviscosity plots for the lower alkanes, propane through hexane, give an activation energy of 3.5 kcal/mol in good agreement with the isolated molecule value. However when the higher members of the alkane series (up to hexadecane) are used in isoviscosity plots, the barrier increases to a value of 4.0 kcal/mol (see Table VII).[154] This trend is opposite to that expected if the energy barrier were being lowered as a result of solvation, since the higher members of the alkane series are more polarizable. The disagreement between the pressure studies and the other methods may suggest a pressure dependence of the barrier; however, similar activation energies were obtained by these workers over different pressure and temperature ranges. The transition state theory approach of Saltiel[155] yields an intrinsic activation enthalpy of 2.9 kcal/mol, which is intermediate to the other two approaches.

The separation of the barrier from the friction effects is surely not rigorous. The limitations are evident in the studies discussed above. Waldeck and co-workers[154,167] observe a variation in activation energies from isoviscosity plots in alkanes. They have studied a series of 4,4'-dialkylstilbenes and find that the variation of the barrier energy becomes more severe for the larger solute molecules (see Table VII). Once again spectral shifts would indicate a trend opposite to that observed through the series.[154] Furthermore if the changing barrier with the solvent range resulted from the inadequacy of the DSE approximation to the friction in the isoviscosity plots, one would expect the larger solute molecules to show less of a trend. It is well-known that as the size of the solute becomes large with respect to the solvent the continuum approximation for the friction becomes quite good.[168] These studies indicate that the solvent does modify the activation barrier.

A variation in the activation energy for reaction with the friction is not in keeping with the one-dimensional model proposed by Kramers. A generalization of the stochastic view to multiple dimensions or the inclusion of memory effects, through the GLE, can provide such an effect. Although the energy barrier, or potential energy surface, does not change in the models, the apparent energy barrier, i.e. activation energy, can change. As suggested by Agmon and Kosloff,[132,136] in the multidimensional case the reaction coordinate may change with the solvent friction. Park and Waldeck[154] proposed that this effect could lead to a change in the measured activation energy for the alkylstilbenes. Schroeder et al.[109] have fit data over a wide range of friction to Kramers' model and find that they must change the effective barrier frequency in different solvents at constant activation energy. They explain this change in the barrier frequency through a multidimensional view of the reaction. Presumably this effect could also be explained by a frequency-dependent friction. Although experimental evidence is consistent with a multidimensional view, conclusive evidence is not yet available.

b. Friction Dependence. Despite these questions about the barrier in solvated systems, it can be instructive to proceed with an analysis of the reduced isomerization rate. Once a barrier is chosen (identified) it is possible to extract the preexponential factor from the expression for the rate constant (eq 8). This re-

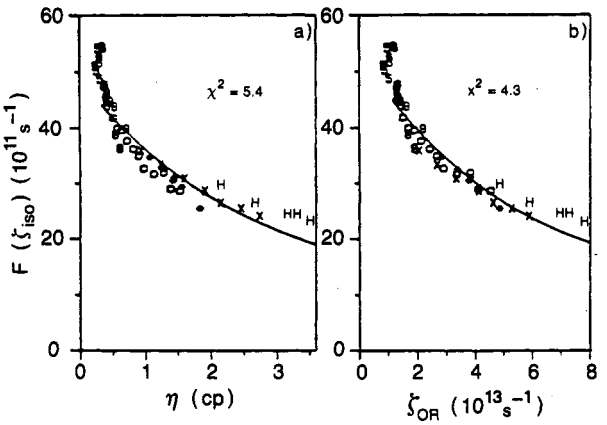

Figure 17. Reduced isomerization rates for *trans*-stilbene in the *n*-alkanes solvents [pentane (5), hexane (6), octane (8), decane (0), dodecane (*), tetradecane (X), and hexadecane (H)] are plotted versus the shear viscosity in a and versus the angular momentum correlation frequency in b. Reproduced from ref 153. Copyright 1988 American Chemical Society.

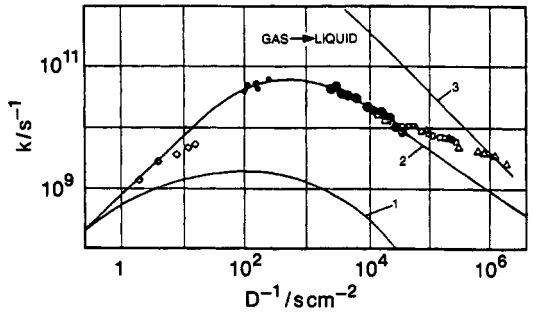

Figure 18. Isomerization rates of *trans*-stilbene are plotted versus the inverse of the diffusion constant in alkane solvents [gaseous methane (◇), gaseous ethane (●), liquid ethane (•), liquid alkanes (□), and compressed hexane (△)]. Curve 1 is the prediction of "standard" RRKM theory and curve 2 is the same model with a modified barrier. Curve 3 represents the rates for isomerization in alcohol solvents. Reproduced from ref 106b. Copyright 1986 American Chemical Society.

duced rate constant can be compared with model predictions. For stilbene the focus has been to study the friction dependence of the reduced rate constant $F(\zeta)$.

Comprehensive studies of *trans*-stilbene isomerization in alkanes have been performed by four groups.[77,106,108,109,128,153,157,160] It is apparent that the hydrodynamic Kramers equation (eq 16) does not adequately model the friction dependence. The predicted line does not curve enough to fit the data (see Figures 17 and 18). The possible importance of frequency-dependent-friction effects had been suggested previously by both theoretical and experimental work. Rothenberger et al.[160] found that the use of a frequency-dependent viscosity could bring the stilbene data into agreement with the Grote–Hynes prediction. As they pointed out, the problem with this approach is that unrealistically small frequencies are obtained for the barrier. The importance of the frequency-dependent solvent friction to the isomerization has been difficult to evaluate for two reasons: (1) most of the rate data spans a relatively narrow friction window and (2) the validity of different models for the frequency dependent friction is unclear.

This same deviation from the Kramers prediction has been observed in other systems as well.[1,125,127] A possible explanation for this behavior is that the shear viscosity of the solvent does not adequately represent the friction experienced by the solute from the solvent. Both spatial and temporal mismatches between the zero-frequency shear viscosity and the size and time scale of the solute motion could be important. In the studies here this problem is exacerbated by the use of different members (pentane through hexadecane) of the homologous series. This mismatch can be considerably reduced by using measured diffusion constants (both rotational and translational) of the solute in the solvent of interest. Lee et al.[77,128] found that using the measured rotational diffusion time of *trans*-stilbene in the particular alkane as a measure of the friction led to good agreement between the measured rates and the Kramers prediction for room temperature data. Subsequently, Kim and Fleming[153] performed a more comprehensive study where both solvent and temperature were varied. They observed an improvement in the agreement between the data and the Kramers prediction when the rotational diffusion time is used as a measure of the friction, but still observe significant deviations, as shown by Figure 17. Clearly the proper modeling of the friction is important in evaluating the adequacy of a one-dimensional Kramers model.

Studies in other systems find a range of behavior as well. For the dye molecule DODCI[125] the use of a rotational diffusion constant instead of the shear viscosity of the solvent has no effect on the size of the deviations from Kramers predictions, whereas the use of diffusion coefficients in the modeling of binaphthyl isomerization[127] brings the rates into agreement with Kramers predictions. More recently Saltiel and Sun[126] have proposed using the translational diffusion coefficient of the moving moiety to model the friction. They model the diffusion coefficient in a manner proposed by Spernol and Wirtz.[169] In this model the friction can be evaluated from bulk-solvent properties and the sizes of the solute and the solvent. The use of this microviscosity for the friction leads to a barrier height of 2.9 kcal/mol and brings the friction dependence of the *trans*-stilbene isomerization into agreement with a one-dimensional Kramers form.

It is well-known that a continuum approximation to the friction experienced by a solute undergoing rotational diffusion in a *single* solvent is quite good, i.e. a proportionality between D^{-1} and η/T holds for a single solvent.[170] Kim and Fleming[153] exploited this behavior in their study of stilbene isomerization in decane and Schroeder et al.[109] exploited this relationship in their studies in ethane through butane. It appears that the deviations from the Kramers predictions, although present, are less severe in these cases. Although this decrease could result from an improvement in the modeling of the friction, in some cases it may reflect a decrease in the range of viscosity studied.

The studies described in these paragraphs indicate that the testing of statistical models with experimental observations is not always clear. The modeling of the solute/solvent friction can become a crucial issue in quantitatively addressing different models. Yet it should be realized that models which are based on the GLE result in a Kramers form for the rate in which the friction constant is replaced by a frequency-dependent friction. Therefore, the need for a better frictional measure in the Kramers equation may indicate the in-

TABLE VIII. Summary of Isomerization Data

system[a]	barrier height, kcal/mol	prefactor at 1 cP, ps^{-1}	a	ref
stilbene				
alkanes	3.5–4.0	3.5–8.1	0.32	153
alcohols	<1	0.02–0.3	0.6	163
nitriles	2.6	1.1	0.51	141
thermal vapor	3.3	0.4		150
stiff stilbene	1.5	1.2	1.0	67
4,4′-DMS				
alkanes	4.3	3.2	0.26	154
4,4′-BuS				
alkanes	4.7	4.5	0.33	167
4,4′-DHS				
alcohols	2.1	0.23	0.61	141
nitriles	4.0	1.0	0.48	141
4,4′-DMeOS				
alkanes	5.7	6.1	0.22	120
alcohols	2.8	0.34	0.67	120
nitriles	4.2	1.4	0.44	141

[a] Stiff stilbene = 1,1′-biinylidene (4); 4,4′-DMS is 4,4′-dimethylstilbene; 4,4′-t-BuS is 4,4′-*tert*-butylstilbene; 4,4′-DHS is 4,4′-dihydroxystilbene; 4,4′-DMeOS is 4,4′-dimethoxystilbene.

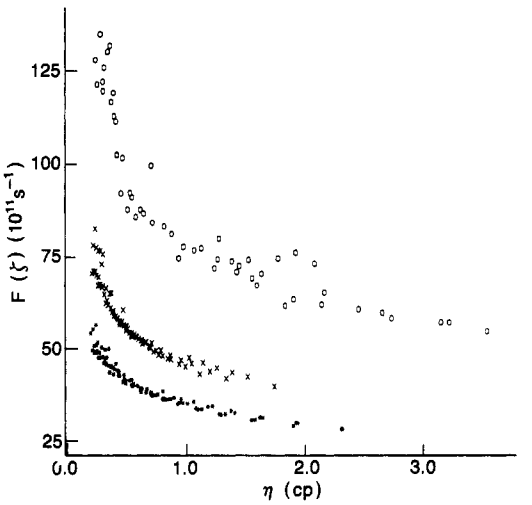

Figure 19. The reduced isomerization rate is plotted versus shear viscosity in *n*-alkane solvents for various solute molecules [(O) *trans*-stilbene, (*) 4,4′-dimethylstilbene, (X) 4,4′-*tert*-butylstilbene).

adequacy of the simple Kramers view. In particular, the use of the diffusion coefficients (rotational and translational) is expected to be a better measure of the friction because it is an empirical probe of the solute/solvent friction on time and space scales which more closely approximate those of the frequency-dependent friction required in the generalized Kramers expression, than does the zero-frequency shear viscosity. On the other hand, most studies of isomerization rates in the high-friction limit probe a dynamic range in rate constant of less than 1 order of magnitude. The two and three parameter fits of the data to the friction dependences predicted by these models may or may not reflect their adequacy.

Studies on model stilbene systems and stilbene derivatives have also been performed. Hochstrasser and co-workers[77,160] studied the viscosity dependence of 1,1′-biindanylidene (compound 4) in *n*-alkanes. This "rigid" version of stilbene has an isomerization rate which agrees quite well with Kramers model predictions when viscosity is used as a measure of the friction. Because the size of the molecule does not change, this observation suggests that spatial variations in the frictional measure, viscosity, between the members of the alkane series are not severe enough to cause deviations from the Kramers prediction. The isomerization rate of rigid stilbene (1,1′-biindanylidene) is considerably more rapid than stilbene, presumably because the barrier for 4 is 1.5 kcal/mol[67] compared to 3.5 kcal/mol for stilbene. The smaller and flatter barrier causes a drop in the magnitude of the preexponential factor. This decrease in frequency and corresponding improvement in comparison to Kramers' model could mean that it is the temporal mismatch between the shear viscosity and the true measure of the friction which is most important for comparisons with the isomerization rates. On the other hand, the reaction coordinate for the "rigid" stilbene may more closely approximate a one-dimensional system.

All of the data can be fit to a power law viscosity dependence (eq 21). Free volume models of the solvent friction, useful in the theory of glasses,[171] were used in the earliest studies[68] to explain the observed friction dependence of the rate. More recently Waldeck and co-workers[120,154] have studied the viscosity dependence of the isomerization rates of different stilbene derivatives in alkanes (see Table VIII). The power, a, in these fits should increase in proportion to the increasing size of the isomerizing moiety, and clearly it does not. The value of the power for *tert*-butyl-substituted stilbene should be twice that of stilbene. Although the strength of the friction dependence (as measured by a) through the series of the *n*-alkanes is in disagreement with this model, the overall rate is reduced over that of *trans*-stilbene as predicted by this model (see Figure 19). The drop in k_{iso} as the size of the isomerizing moiety increases reflects more the change in activation energy than in preexponential factor. In fact, in Figure 19, the reduced isomerization rate for *tert*-butyl-substituted stilbene is larger than that for the methylated species. This anomaly could very easily arise from uncertainty in the barrier heights, but may reflect the importance of methyl torsion to the reaction coordinate. The method proposed by Saltiel[67,126,155] for separating the barrier and viscosity effects provides a more consistent set of a values. That analysis will be presented elsewhere.[166]

Park and Waldeck[154] have proposed that the weaker viscosity dependence observed for the isomerization of 4,4′-dimethylstilbene than of *trans*-stilbene can be explained by multidimensional effects. For the dimethyl species the methyl rotor states mix with the low-frequency torsional modes[34] of the phenyl rings. This increased coupling to modes orthogonal to the reaction coordinate could account for an increased importance of multidimensional effects in the methyl species. The trends in the friction dependence could result from two quite different effects. The first was proposed by Agmon and Kosloff[132] who allow for two pathways to go from reactant to product. These pathways have different friction dependences and energy barriers, such that changing the viscosity (friction) of the medium changes the relative rates of these two competing pathways. Alternatively these friction effects could be created by coupling between the reactive and nonreactive modes. The mechanism here is more akin to an internal friction. Coalson and Chen[134b] have shown that the trend in the experimental results for *trans*-

stilbene and 4,4'-dimethylstilbene can be accounted for in this manner. This evidence pointing toward multidimensional effects is circumstantial at best, and is complicated by variations in the potential energy surface between the solutes and through the solvent series. Lastly, as discussed earlier, studies of *m*-methylstilbenes are suggestive of a competition between the overall isomerization and phenyl torsional motion.[33]

It is important to realize that the friction studies show relatively small differences (~20%) between the Kramers model prediction and experiment, i.e. this simple model provides a reasonable estimate of the rates. Whether the deviations are more severe requires the study of the high-friction rate over a *wider* viscosity range, preferably by the variation of temperature and pressure. The small differences found so far between the model and the data suggest that friction dependences may not be the best probe of the limits of the Kramers picture.

c. cis-Stilbene. Monitoring the isomerization dynamics of *cis*-stilbene is considerably more challenging, but recent technological advances have made this possible. Three groups[56,73-76] have begun probing the dynamics of this reaction. The general features are a rapid rate, a few picoseconds at most, and a weak solvent dependence. Petek et al.[75,76] have probed the decay of *cis*-stilbene and the appearance of *trans*-stilbene in rare gas clusters. As described previously, they identify the importance of the DPH channel in the decay of *cis*-stilbene and their studies reveal the rapid and nonexponential relaxation of the initially created cis population. Abrash et al.[56] have monitored the decay of cis and the appearance of *trans*-stilbene in solution by transient-absorption methods. They have identified new spectral features associated with the cis species and obtained rates. They find that the ground-state trans isomer begins to appear within 150 fs after the creation of the cis excited state. The viscosity dependence of the rates is weaker than that of the *trans*-stilbene case and can be fit to the Kramers expression by using a rotational diffusion coefficient as a measure of the friction. The form and time scale of the observed transients indicate that the initially created distribution of cis species occurs on a flat part of the potential. Todd et al.[73] have studied the cis isomer by using fluorescence methods. The population studies are generally in agreement with the observations of Abrash, and the viscosity dependence is found to be weak. With depolarized fluorescence methods these workers place restrictions on the reaction coordinate similar to those found by Abrash et al.[56] They also find that the excited state decay rate decreases significantly upon deuteration and interpret this change as indicating the importance of ethylenic hydrogen motions on the reaction coordinate.

The primary difference between the reaction dynamics of the cis and trans isomers is the lack of a barrier for the cis species. This makes the measured dynamics a function of the preparation step which may eventually allow considerably more detail to be obtained for the excited-state dynamics. In particular because of the rapid reaction rate the effects of vibrational redistribution, intramolecular and intermolecular, should be important. A recent study by Sension et al.[177] reports that the product of the cis isomerization is formed vibrationally hot. The cis studies also reveal the rapid appearance of the product species in the ground state. If the intermediate ("phantom") state is a common one, then the irreversibility of the initial twisting for the trans species is assured. Recently, Saltiel and coworkers[41] reported that the formation of excited *trans*-stilbene from the excited *cis*-stilbene, i.e. the back reaction, occurs but is small.

2. Polar Solvents

The discussion of isomerization in polar solvents will be divided into two components: (1) *trans*-stilbene and nonpolar stilbenes and (2) polar stilbenes. When the initially excited stilbene has a dipole moment or donor and acceptor groups, the initial trans state creates a polarization field in the solvent which complicates the reaction dynamics.[120] For the case of nonpolar stilbenes the primary effect of solvent polarity will be on the transition-state energy. For studies in polar solvents the extraction of a reaction barrier is much more complicated than in the alkane solvents, and in some cases may not be possible at all.

a. Nonpolar Stilbenes. For nonpolar solutes the activation energy for the reaction in a polar solvent is observed to decrease when compared to the corresponding value in alkane solvent. Studies of stilbene and its symmetrically substituted analogues have been performed in two homologous series of solvents, *n*-alkanenitriles[141] and *n*-alkyl alcohols,[120,141,163-165] as well as numerous other solvents.[162,172] The decrease of the activation energy suggests that the transition state is polar and/or polarizable, in agreement with the expectation from electronic structure considerations, i.e. the importance of the doubly excited configuration.

In the *n*-alkanenitrile solvents, from propanenitrile to decanenitrile, isoviscosity plots yield constant slopes over a range of viscosities (0.7–5.0 cP). The activation energy for the isomerization of *trans*-stilbene is 2.4 kcal/mol, significantly lower than the value observed in *n*-alkane solvents, but still somewhat higher than the barriers found by Troe and co-workers in ethane through butane solvents. Because a barrier can be identified, albeit a solvated barrier, it is possible to examine the reduced isomerization rates. As with the alkane case, it is found that the hydrodynamic Kramers form is inadequate for describing the rates throughout the homologous series and even for particular members of the series.[141b] Waldeck and co-workers[141] have compared their rate constant data to a variety of models. They find the best agreement with a coupled oscillator model proposed by van der Zwan and Hynes.[137] The results of fitting the stilbene rates to that model are shown in Figure 20. Although the agreement is very good (within a few percent), it is possible to see systematic deviations of the data in particular solvents. These workers have also examined 4,4-dimethoxystilbene and 4,4-dihydroxystilbene in the *n*-alkanenitriles and make similar observations. With the model of van der Zwan and Hynes,[137] it is possible to rescale the reduced isomerization rates by dividing through with the barrier frequency. A plot of the scaled rates for the three solutes studied is shown in Figure 21. In this plot the best fit barrier frequency of 26 cm^{-1} is used for *trans*-stilbene.[141] The scaling parameter which accounts for the change in barrier frequency for the other

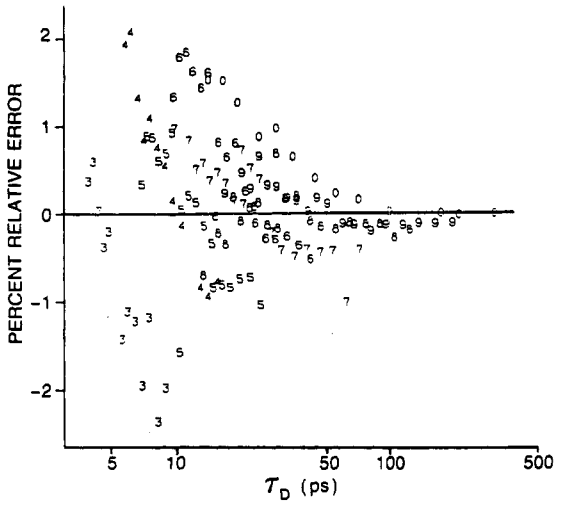

Figure 20. A plot of the percent deviation of the reduced isomerization rate from the coupled oscillator model of van der Zwan and Hynes[137] is plotted versus the Debye relaxation time of the solvent for *trans*-stilbene in the *n*-alkanenitriles. Each number in the plot is the number of carbon atoms in the solvent molecule except for decanenitrile, which is represented by a 0. Reproduced from ref 141b. Copyright 1989 American Institute of Physics.

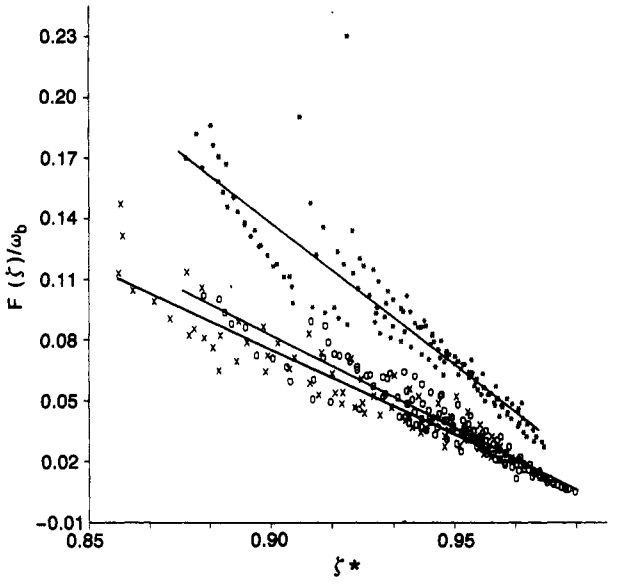

Figure 21. The reduced isomerization rates of *trans*-stilbene (O), 4,4′-dihydroxystilbene (X), and 4,4′-dimethoxystilbene (*) are rescaled and plotted versus the friction ζ^*. This frequency-dependent friction is given by $\zeta^* = F(\zeta)\tau_D/(1 + F(\zeta)\tau_D)$, where τ_D is the Debye relaxation time of the solvent. The lines are best fits to the coupled oscillator model.

solutes is obtained by using their measured activation energies and estimating their reduced moments of inertia.[141] The success of the rescaling procedure suggests that the primary influences on the rate have been included. The change in slope between these plots can be interpreted as a variation in the solute/solvent coupling strength. The comparison of the data with this model rests on the ability to identify a solvated barrier for the reaction, which has been a problem for the other studies in polar solvents.

The isomerization rate behavior of stilbene has also been examined in the *n*-alkyl alcohol solvents.[163-165] In this case the attempt to extract an activation barrier fails. The isoviscosity plots are observed to decrease

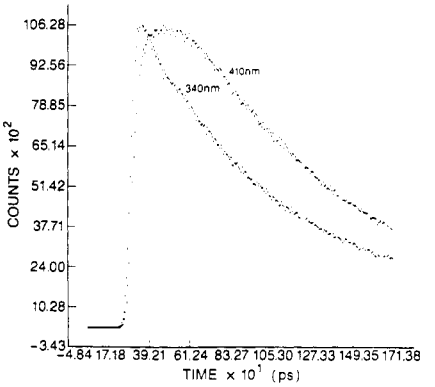

Figure 22. Decay curves for 4,4′-dimethoxystilbene in decanol are shown in two different regions of the fluorescence spectrum. The slower rise time and rounded top of the red emission is the signature of solvent reorganization about the excited state. Reproduced from ref 120. Copyright 1988 American Chemical Society.

in slope as the viscosity increases. This trend corresponds to a decrease in activation energy for the larger members of the alcohol series which are less polar. The use of empirical polarity parameters are unable to compensate for the drift in activation energy. More interestingly these parameters would predict a trend opposite to that observed. The more polar members of the series should better solvate the transition state leading to a decrease in the barrier height as the polarity increases. Hicks et al.[164] suggested that a dynamic polarity effect may be at work in this case.

Similar behavior to that in *trans*-stilbene was found for 4,4-dimethoxystilbene and 4,4-dihydroxystilbene by Waldeck and co-workers.[120,141] Because the intrinsic reaction barrier appears to be higher in these compounds and the Stokes shift is larger, they were able to observe the interplay of solvation dynamics and reaction at early times (see Figure 22). The figure shows that the blue portion of the spectrum appears immediately and decays away by reaction and solvation, whereas the red portion of the spectrum grows with solvation as it decays away by reaction. The nonexponentiality in the population decay curves reflects this dynamics. Rate constants can be extracted from the data by fitting the decays at long times and these are used in isoviscosity plots. If isoviscosity plots are used for *n*-alcohols from propanol to decanol, there is little variation in the slope. The activation energies for the *n*-alcohols in Table VIII correspond to this case. In the stilbene case the decay rate and solvation rates strongly overlap in time, making the analysis somewhat more complicated.

The view proposed by Waldeck[120,141a] to explain the inverted trend in isoviscosity plots relies on nonequilibrium solvation effects. It is useful to consider three time scales. First is the phenomenological or laboratory time scale determined by the fluorescence decay time. For 4,4-dimethoxystilbene this ranges from 100 ps to the nanosecond regime. Second is the solvation time scale, known to be dispersive in alcohol solvents,[173] which ranges from a picosecond or less in methanol to about 100 ps in decanol at room temperature. Because the decay of population is slow with respect to solvation, the members of the ensemble at long times (where the decay rate constants are extracted) are equilibrium solvated as reactants. The trend in solvation energy

should reflect the trend in Stokes shift between the different members of the series (200 cm^{-1} for methanol decreasing to 50 cm^{-1} for decanol), so that the reactant has a lower energy in the more polar solvent than in the less polar solvent. The third time scale is the reactive time scale, or time scale defined by the reduced isomerization rate, which is probably a picosecond or less, by analogy to the alkane data. This time scale is more rapid than solvation so that the solvation of the transition state is not complete. One manner of measuring this solvation would be to determine the dielectric response of the medium on the reactive time scale. Dielectric constants of the alcohols are not available in this frequency regime, but the overall trend is that the dielectric response of the different alcohols become similar as the frequency of the applied electric field is increased. Eventually the order of polarity inverts in the series, i.e. decanol has a higher index of refraction than does methanol. If the solvation of the transition state for different members of the series is similar because the sluggish nuclear degrees of freedom of the solvent are "frozen out", then the more polar members of the solvent would appear to have higher activation energies because the solute began in a stronger solvent-polarization field. This perspective provides a consistent and qualitative explanation for the observed trend.

An alternative perspective is similar to a model proposed by Marcus and Sumi[133] for electron-transfer reactions. In this model a two-dimensional representation of the free energy surface of the true many-dimensional solute/solvent energy surface is used. One coordinate is an internal reactive coordinate of the solute and the second coordinate is a solvent-polarization coordinate. Reaction proceeds by motion from the reactant well to the product well and relies explicitly on the solvent polarization. This view can also be used to qualitatively explain the observations of isomerization rates in alcohols.[141a] More recent models of dynamical effects in polar solvents are available and it may soon be possible to quantitate the rate behavior in these complicated polar solvents.

As alluded to above, many studies have been performed in nonhomologous sets of solvents, making it somewhat more difficult to identify trends. In all cases the isomerization rates are found to depend on the solvent polarity. In general the conclusions given above are consistent with these observations.

The studies in the polar solvents rely on the method of extracting the activation barrier in the homologous series. As discussed, the rigor of this method is questionable. In order to identify a barrier the solvents studied should have two attributes: (1) the change in polarity, despite how it is measured, should vary little through the series and (2) the time scale of solvation should be similar through the series.[173,174] Whether the barriers extracted correspond to equilibrium solvated barriers, as described by van der Zwan and Hynes, is not known. A much better method of identifying barriers to reaction would be to perform studies in a single solvent as a function of temperature and pressure.

b. Polar Stilbenes. The primary focus for most of the studies of asymmetric stilbenes[84-94] has been to define the mechanistics of the isomerization reaction. As mentioned previously, interesting solvent effects are present in these systems, resulting from their dipolar character. Much of the data on the isomerization rates comes from quantum-yield measurements and the dynamical effects of solvation and reaction are not immediately obvious. More recently[93] time-resolved studies have shown the effects of solvation.

The case of donor/acceptor-substituted stilbenes is most dramatic. As the polarity of the solvent increases the isomerization yield may initially increase as is observed with stilbene, but eventually maximizes and starts to decline.[84,88,91,94] Evidence for the presence of a twisted intramolecular charge transfer (TICT) state has been found for 4-(dimethylamino)-4′-cyanostilbene.[93,175] The mechanism for the decrease in quantum yield with increasing polarity may very well be the increase in this nonradiative-decay channel which is competitive with isomerization. The generality of the TICT state for polar stilbenes remains unclear. Whether a TICT state is present or not, the decrease in isomerization yield with polarity could be explained by the model given above for the alcohols. As the polarity increases the solvation energy of the reactant increases. For the polar stilbenes the dipole moment can be very large (32 D in the case of 4-(dialkylamino)-4′-nitrostilbenes[95] which may undergo TICT). Since the polarization field of the solvent is large and presumably sluggish compared to the reactive time scale, the solute can become trapped in the solvent cage. This polarization caging of the reactant increases the activation energy of reaction, causing a significant decrease in the rate. More time-resolved studies are needed to probe the dynamics of these interesting systems.

VII. Conclusions

Stilbene photophysics has been and continues to be an important model for investigating condensed-phase reaction dynamics. The progress on this problem in the past decade has been enormous. This system is one of the few for which a variety of methods has been used to investigate the dynamics from the isolated molecule to the solvated molecule. Much of the spectroscopy and structure of the species has been revealed by the combination of high-resolution spectroscopy and supersonic beam methods. The question of IVR in the isolated molecule has been addressed. Ultrafast absorption, fluorescence, and excited-state Raman spectra of this reaction have been taken for a thermal ensemble. Microcanonical reaction rates have been measured in a jet expansion. The isomerization rate has been observed over the entire friction range. Time-resolved measurements of rates are revealing interesting features of the dynamics and the observation of nonexponential kinetics are probing dynamical features of the reaction directly.

Despite the high level of progress and understanding, questions linger. Why exactly are the rates so different for the isolated molecule and the solvated one? When can IVR be considered complete? What modes are involved in the reaction coordinate? Are multidimensional effects important for the reaction dynamics or is it reasonably modeled as one dimensional? Can the important effects of solvation, both static and dynamic, be quantitated? A combination of theory and experiment will be needed to address these issues. Of critical importance to many of these questions will be knowl-

edge of the potential energy surface, both isolated and solvated.

VIII. Acknowledgments

Support by the National Science Foundation (CHE-8613468) is acknowledged. Preprints of recent work from K. Yoshihara, G. R. Fleming, N. Agmon, and J. Troe are much appreciated. We also thank T. Gustafson, G. R. Fleming, and J. Saltiel for useful comments.

IX. References

(1) (a) Saltiel, J.; D'Agostino, J.; Megarity, E. D.; Metts, L.; Neuberger, K. R.; Wrighton, M.; Zafiriou, O. C. *Organic Photochemistry*; Chapman, O. L., Ed.; Marcel Dekker: New York, 1973; Vol. 3. (b) Saltiel, J.; Charlton, J. L.; *Rearrangements in Ground and Excited States*; Mayo, Ed.; Academic Press: New York, 1980; Vol. 3.
(2) Saltiel, J.; Sun, Y. P. *Photochromism-Molecules and Systems*; Dürr, H., Bouas-Laurent, H., Eds.; Elsevier: Amsterdam, 1990; p 64.
(3) Hochstrasser, R. *Pure Appl. Chem.* **1980**, *52*, 2683.
(4) Fleming, G. R. *Chemical Applications of Ultrafast Spectroscopy*; Oxford: New York, 1986.
(5) Saltiel, J. *J. Am. Chem. Soc.* **1967**, *89*, 1036.
(6) Albert, I. D. L.; Ramasecha, S. *J. Phys. Chem.* **1990**, *94*, 6540.
(7) Salem, L. *Electrons in Chemical Reactions*; Wiley: New York, 1982.
(8) Orlandi G.; Siebrand, W. *Chem. Phys. Lett.* **1975**, *30*, 352.
(9) Troe, J.; Weitzel, K. M. *J. Chem. Phys.* **1988**, *88*, 7030 and references therein.
(10) Gregory, A. R.; Williams, D. F. *J. Phys. Chem.* **1979**, *83*, 2652 and references therein.
(11) (a) Orlandi, G.; Palmieri, P.; Poggi, G. *J. Am. Chem. Soc.* **1979**, *101*, 3492. (b) Negri, F.; Orlandi, G.; Zerbetto, F. *J. Phys. Chem.* **1989**, *93*, 5124 and references therein.
(12) Klein, M.; Buss, V. *Chem. Phys. Lett.* **1986**, *123*, 509.
(13) Warshel, A. *J. Chem. Phys.* **1975**, *62*, 214.
(14) Stachelek, T. M.; Pazoha, T. A.; McClain, W. M.; Drucker, R. P. *J. Chem. Phys.* **1977**, *66*, 4540.
(15) Fuke, K.; Sakamato, S. A.; Ueda, M.; Itoh, M. *Chem. Phys. Lett.* **1980**, *74*, 546.
(16) Hohlneicher, G.; Dick, B. *J. Photochem.* **1984**, *27*, 215.
(17) Burrow, P. D.; Michejda, J. A.; Jordan, K. D. *J. Chem. Phys.* **1987**, *86*, 9.
(18) Champagne, B. B.; Pfanstiel, J. F.; Plusquellic, D. F.; Pratt, D. W.; van Herpen, W. M.; Meerts, W. L. *J. Phys. Chem.* **1990**, *94*, 6.
(19) (a) Urano, T.; Hamaguchi, H.; Tasumi, M.; Yamanouchi, K.; Tsuchiya, S. *Chem. Phys. Lett.* **1987**, *137*, 559. (b) Urano, T.; Hamaguchi, H.; Tasumi, M.; Yamanouchi, K.; Tsuchiya, S.; Gustafson, T. L. *J. Chem. Phys.* **1989**, *91*, 3884. (c) Urano, T.; Maegawa, M.; Yamanouchi, K.; Tsuchiya, S. *J. Phys. Chem.* **1989**, *89*, 3459.
(20) Syage, J. A.; Felker, P. M.; Zewail, A. H. *J. Chem. Phys.* **1984**, *81*, 4685.
(21) (a) Zwier, T. S.; Carrasquillo, E. M.; Levy, D. H. *J. Chem. Phys.* **1983**, *78*, 5493. (b) Spangler, L. H.; van Zee, R.; Zwier, T. S. *J. Phys. Chem.* **1987**, *91*, 2782.
(22) Dyck, R. H.; McClure, D. S. *J. Chem. Phys.* **1962**, *36*, 2326.
(23) (a) Suzuki, T.; Mikami, N.; Ito, M. *J. Phys. Chem.* **1986**, *90*, 6431. (b) Ito, M. *J. Phys. Chem.* **1987**, *91*, 517.
(24) Baranovic, G.; Meic, Z.; Gusten, H.; Mink, H.; Keresztury, G. *J. Phys. Chem.* **1990**, *94*, 2833.
(25) (a) Meic, Z.; Gusten, H. *Spect. Acta* **1978**, *34A*, 101. (b) Meic, Z.; Baranovic, G.; Skare, D. *J. Mol. Struct.* **1986**, *141*, 375.
(26) Bree, A.; Edelman, M. *Chem. Phys.* **1980**, *51*, 77.
(27) (a) Hamaguchi, H. *J. Chem. Phys.* **1988**, *89*, 2587. (b) Hamaguchi, H. *Chem. Phys. Lett.* **1986**, *126*, 185. (c) Hamaguchi, H. *Vibrational Spectra and Structure*; During, J. R., Ed.; Elsevier: New York, 1986; Vol. 16.
(28) (a) Gustafson, T. L.; Roberts, D. M.; Chernoff, D. A. *J. Chem. Phys.* **1983**, *79*, 1559. (b) *Ibid.* **1984**, *81*, 3438. (c) Gustafson, T. L.; Chernoff, D. A.; Palmer, J. F.; Roberts, D. M. *Time Resolved Raman Spectroscopy*; Atkinson, G. H., Maeda, S., Eds.; Gordon and Breach: New York, 1986.
(29) Herzberg, G. *Infrared and Raman Spectra*; van Nostrand: New York, 1945.
(30) (a) Hoekstra, A.; Meertens, P.; Vos, A. *Acta Crystallogr.* **1975**, *B31*, 2813. (b) Finder, C. J.; Newton, M. G.; Allinger, N. L. *Acta Crystallogr.* **1974**, *B30*, 411. (c) Bernstein, J. *Acta Crystallogr.* **1975**, *B31*, 1268.
(31) Traetteberg, M.; Frantsen, E. B.; Mijlhoff, F. C.; Hoekstra, A. *J. Mol. Struct.* **1975**, *26*, 57.
(32) Kobayashi, T.; Suzuki, H.; Ogawa, K. *Bull. Chem. Soc. Jpn.* **1982**, *55*, 1734.
(33) Park, N. S.; Waldeck, D. H. *Chem. Phys. Lett.* **1990**, *168*, 379.
(34) Spangler, L. H.; Bosman, W. B.; van Zee, R. D.; Zwier, T. S. *J. Chem. Phys.* **1988**, *88*, 6768.
(35) Frederick, J. H.; Fujiwara, Y.; Penn, J. H.; Yoshihara, K.; Petek, H. *J. Phys. Chem.*, in press.
(36) (a) Greene, B. I.; Hochstrasser, R. M.; Weisman, R. B. *Chem. Phys.* **1980**, *48*, 289. (b) *Ibid. J. Chem. Phys.* **1979**, *71*, 544.
(37) (a) Fischer, E. *J. Mol. Struct.* **1982**, *84*, 219. (b) Fischer, E. *J. Phys. Chem.* **1980**, *84*, 403. (c) Fischer, E. *J. Photochem.* **1981**, *17*, 331.
(38) Higuchi, J.; Ishizu, K.; Nemoto, F.; Tajima, K.; Suzuki, H.; Ogawa, K. *J. Am. Chem. Soc.* **1984**, *106*, 5403.
(39) (a) Zwier, T. S. *J. Chem. Phys.* **1989**, *90*, 3967. (b) DeHaan, D. O.; Holton, A. L.; Zwier, T. S. *J. Chem. Phys.* **1989**, *90*, 3952. (c) Bahatt, D.; Even, U.; Jortner, J. *Chem. Phys. Lett.* **1985**, *117*, 527.
(40) Petek, H.; Fujiwara, Y.; Kim, D.; Yoshihara, K. *J. Am. Chem. Soc.* **1988**, *110*, 6269.
(41) Saltiel, J.; Waller, A.; Sun, Y. P.; Sears, D. F., Jr. *J. Am. Chem. Soc.* **1990**, *112*, 4580.
(42) (a) Malkin, S.; Fischer, E. *J. Phys. Chem.* **1964**, *68*, 1153. (b) Fischer, G.; Seger, G.; Muszkat, K. A.; Fischer, E. *J. Chem. Soc., Perkins. Trans. 2* **1975**, 1569. (c) Goedicke, C.; Stegemeyer, H.; Fischer, G.; Fischer, E. *Z. Phys. Chem.* **1976**, *101*, 181. (d) Sharafy, S.; Muszkat, K. A. *J. Am. Chem. Soc.* **1971**, *93*, 4119.
(43) Yoshihara, K.; Namiki, A.; Sumitani, M.; Nakashima, N. *J. Chem. Phys.* **1979**, *71*, 2892.
(44) Traetteberg, M.; Frantsen, E. B. *J. Mol. Struct.* **1975**, *26*, 69.
(45) *Theory and Applications of Ultraviolet Spectroscopy*; Jaffé, H. H., Orchin, M., Eds.; Wiley: New York, 1962.
(46) *Techniques of Chemistry III: Photochromism*; Brown, G. H., Ed.; Wiley: New York, 1971.
(47) (a) Bolotnikova, T. N.; Malkes, L. Y.; Nazarenko, A. I.; Yakovenko, V. N. *Opt. Spekt.* **1968**, *25*, 621. (b) *Ibid.* **1969**, *26*, 132. (c) *Ibid.* **1969**, *26*, 649.
(48) (a) Pavloupos, T. G.; Taylor, D. G., III *Spectrochim. Acta* **1985**, *1383*, 1357. (b) Ikeyama, T.; Azumi, T. *J. Phys. Chem.* **1988**, *92*.
(49) (a) Saltiel, J.; D'Agostino, J. T.; Herkstroeter, W. G.; Saint-Ruf, G.; Buu-Hoi, N. P. *J. Am. Chem. Soc.* **1973**, *95*, 2543. (b) Herkstroeter, W. G.; McClure, D. S. *J. Am. Chem. Soc.* **1968**, *90*, 4522.
(50) (a) Heinrich, G.; Blume, H.; Schulte-Frohlinde, D. *Tetrahedron Lett.* **1967**, *47*, 4693. (b) Heinrich, G.; Holzer, G.; Blume, H.; Schulte-Frohlinde, D. *Z. Naturforsch.* **1970**, *25b*, 496.
(51) Langkilde, F. W.; Wilbrandt, R.; Negri, F.; Orlandi, G. *Chem. Phys. Lett.* **1990**, *165*, 66.
(52) Gorner, H. *J. Phys. Chem.* **1989**, *93*, 1826.
(53) Greene, B. I.; Hochstrasser, R. M.; Weisman, R. B. *Chem. Phys. Lett.* **1979**, *62*, 427.
(54) Teschke, O.; Ippen, E. P.; Holtom, G. R. *Chem. Phys. Lett.* **1977**, *52*, 233.
(55) (a) Sumitani, M.; Yoshihara, K. *J. Chem. Phys.* **1982**, *76*, 738. (b) Petek, H.; Yoshihara, K. *J. Chem. Phys.* **1987**, *87*, 1458.
(56) Abrash, S.; Repinec, S.; Hochstrasser, R. M. *J. Chem. Phys.* **1990**, *93*, 1041.
(57) (a) Hopkins, J. B.; Rentzepis, P. M. *Chem. Phys. Lett.* **1986**, *124*, 79. (b) Payne, S. A.; Hochstrasser, R. M. *J. Phys. Chem.* **1986**, *90*, 2068. (c) Kamalov, V. F.; Koroteev, N. I.; Shkurinov, A. P.; Toleutaev, B. N. *Chem. Phys. Lett.* **1988**, *147*, 335.
(58) Myers, A. B.; Trulson, M. O.; Mathies, R. A. *J. Chem. Phys.* **1985**, *83*, 5000.
(59) Myers, A. B.; Mathies, R. A. *J. Chem. Phys.* **1984**, *81*, 1552.
(60) Oki, M.; Kunimoto, H. *Spectrochim. Acta* **1963**, *19*, 1463.
(61) Laarhoven, W. H.; Nivard, R. J. F.; Havinga, E. *Rec. Trav. Chim. Pays-Bas* **1960**, *79*, 1153.
(62) Beale, R. N.; Roe, E. M. F. *J. Chem. Soc.* **1952**, *74*, 2302.
(63) Muszkat, K. A.; Fischer, E. *J. Chem. Soc. B* **1967**, 662.
(64) Stermitz, F. R. *Organic Photochemistry*; Chapman, O. L., Ed.; Marcel Dekker: New York, 1967; Vol. 1. (b) Mallory, F. B.; Mallory, C. W. *Organic Reactions*; Wiley: New York, 1983; Vol. 30, p 1. (c) Laarhoven, W. H. *Recl. Trav. Chim. Pays-Bas* **1983**, *102*, 241.
(65) (a) Saltiel, J.; Marchand, G. R.; Kirkor-Kaminska, E.; Smothers, W. K.; Mueller, W. B.; Charlton, J. L. *J. Am. Chem. Soc.* **1984**, *106*, 3144. (b) Saltiel, J.; Ganapathy, S.; Werking, C. *J. Phys. Chem.* **1987**, *91*, 2755. (c) Saltiel, J.; Rousseau, A. D.; Thomas, B. *J. Am. Chem. Soc.* **1983**, *105*, 7631.
(66) Malkin, S.; Fischer, E. *J. Phys. Chem.* **1962**, *66*, 2482.
(67) Saltiel, J.; D'Agostino, J. T. *J. Am. Chem. Soc.* **1972**, *94*, 6445.
(68) (a) Gegiou, D.; Muszkat, K. A.; Fischer, E. *J. Am. Chem. Soc.* **1968**, *90*, 12. (b) Gegiou, D.; Muszkat, K. A.; Fischer, E. *J. Am. Chem. Soc.* **1968**, *90*, 3907.
(69) Brey, L. A.; Schuster, G. B.; Drickamer, H. G. *J. Am. Chem. Soc.* **1979**, *101*, 129.

(70) (a) Saltiel, J. *J. Am. Chem. Soc.* **1968**, *90*, 6394. (b) Hammond, G. S.; Saltiel, J.; Lamola, A. A.; Turro, N. J.; Bradshaw, J. S.; Cowan, D. O.; Counsell, R. C.; Vogt, V.; Dalton, C. *J. Am. Chem. Soc.* **1964**, *86*, 3197.
(71) Sumitani, M.; Yoshihara, K. *Bull. Chem. Soc. Jpn.* **1982**, *55*, 85.
(72) (a) Greene, B. I.; Scott, T. W. *Chem. Phys. Lett.* **1984**, *106*, 399. (b) Greene, B. I.; Farrow, R. C. *J. Chem. Phys.* **1983**, *78*, 3336.
(73) Todd, D. C.; Jean, J. M.; Rosenthal, S. J.; Ruggiero, A. J.; Yang, D.; Fleming, G. R. *J. Chem. Phys.* **1990**, *93*, 8658.
(74) (a) Doany, F. E.; Hochstrasser, R. M.; Greene, B. I.; Millard, R. R. *Chem. Phys. Lett.* **1985**, *118*, 1. (b) Doany, F. E.; Heilweil, E. J.; Moore, R.; Hochstrasser, R. M. *J. Chem. Phys.* **1984**, *80*, 201.
(75) (a) Sumitani, M.; Nakashima, N.; Yoshihara, K. *Chem. Phys. Lett.* **1979**, *68*, 255. (b) Petek, H.; Yoshihara, K.; Fujiwara, Y.; Frey, J. G. *J. Opt. Soc. Am. B* **1990**, *7*, 1540. (c) Petek, H.; Yoshihara, K.; Fujiwara, Y.; Frey, J. G. *Ultrafast Phenomena VII*; Harris, C. B., Ippen, E. P., Mourou, G. A., Zewail, A. H., Eds.; Springer, New York, 1990.
(76) Petek, H.; Yoshihara, K.; Fujiwara, Y.; Lin, Z. H.; Penn, J. H.; Frederick, J. H. *J. Phys. Chem.* **1990**, *94*, 7539.
(77) Lee, M.; Bain, A. J.; McCarthy, P. J.; Han, C. H. Haseltine, J. N.; Smith, A. B., III; and Hochstrasser, R. M. *J. Chem. Phys.* **1986**, *85*, 4341.
(78) (a) Shim, S. C.; Chae, J. S. *Bull. Chem. Soc. Jpn.* **1982**, *55*, 1310. (b) Saltiel, J.; Zifiriou, O. C.; Megarity, E. D.; Lamola, A. A. *J. Am. Chem. Soc.* **1968**, *90*, 4759. (c) Pyun, C.; Lyle, T. A.; Daub, G. H.; Park, S. M. *Chem. Phys. Lett.* **1986**, *124*, 48.
(79) Courtney, S. H.; Balk, M. W.; Philips, L. A.; Webb, S. P.; Yang, D.; Levy, D. H.; Fleming, G. R. *J. Chem. Phys.* **1988**, *89*, 6697.
(80) Nordholm, S. *Chem. Phys.* **1989**, *137*, 109.
(81) Park, N. S.; Waldeck, D. H. *Ultrafast Phenomena VII*; Harris, C. B., Ippen, E. P., Mourou, G. A., Zewail, A. H., Eds; Springer, New York, 1990.
(82) Matthews, A. C.; Sakurovs, R.; Ghiggino, K. P. *J. Photochem.* **1982**, *19*, 235.
(83) (a) Sun, Y. P.; Sears, D. F., Jr.; Saltiel, J.; Mallory, F. B.; Mallory, C. W.; Bruser, C. A. *J. Am. Chem. Soc.* **1988**, *110*, 6974 and references therein. (b) Shim, S. C.; Lee, K. T.; Kim, M. S. *J. Org. Chem.* **1990**, *55*, 4316.
(84) (a) Gorner, H. *Ber. Bunsen.-Ges. Phys. Chem.* **1984**, *88*, 1199 and references therein. (b) Gorner, H.; Schulte-Frohlinde, D. *Ibid.* 1208. (c) *Ibid.* **1978**, *82*, 1102. (d) Schulte-Frohlinde, D.; Gorner, H. *Pure Appl. Chem.* **1979**, *51*, 279 and references therein.
(85) Gorner, H. *J. Photochem.* **1980**, *13*, 269.
(86) Gorner, H. *J. Photochem. Photobiol.* **1987**, *A40*, 325.
(87) Gorner, H.; Schulte-Frohlinde, D. *J. Phys. Chem.* **1979**, *83*, 3107.
(88) Gorner, H.; Schulte-Frohlinde, D. *J. Mol. Struct.* **1982**, *84*, 227.
(89) Saltiel, J.; Marinari, A.; Chang, D. W. L.; Mitchener, J. C.; Megarity, E. D. *J. Am. Chem. Soc.* **1979**, *101*, 2982.
(90) Pisanias, M. N.; Schulte-Frohlinde, D. *Ber. Bunsen.-Ges. Phys. Chem.* **1975**, *79*, 662.
(91) (a) Gruen, H.; Gorner, H. *Z. Naturforsch.* **1983**, *38A*, 929. (b) Gruen, H.; Gorner, H. *J. Phys. Chem.* **1989**, *93*, 7144. (c) Gorner, H.; Gruen, H. *J. Photochem.* **1985**, *28*, 329.
(92) (a) Gloyna, D.; Gryczynski, I.; Kawski, A. *Z. Naturforsch.* **1981**, *36a*, 626. (b) Gloyna, D.; Kawski, A.; Gryczynski, I. *Z. Naturforsch.* **1982**, *37a*, 383. (c) Gloyna, D.; Kawski, A.; Gryczynski, I.; Cherek, H. *Monatsh. Chem.* **1987**, *118*, 759.
(93) Gilabert, E.; Lapouyade, R.; Rulliere, C. *Chem. Phys. Lett.* **1988**, *145*, 262.
(94) (a) Rettig, W.; Majenz, W. *Chem. Phys. Lett.* **1989**, *154*, 335. (b) Lippert, E.; Rettig, W.; Bonacic-Koutecky, V.; Heisel, F.; Miehe, J. A. *Advances in Chemical Physics*; Rice, S. A., Prigogine, I., Eds.; Wiley: New York, 1987; Vol. 68.
(95) (a) Kawski, A.; Gryczinski, I.; Jung, C.; Heckner, K. H. *Z. Naturforsch.* **1977**, *32a*, 420. (b) Baumann, W.; Deckers, H.; Loosen, K. D.; Petzke, F. *Ber. Bunsen.-Ges. Phys. Chem.* **1977**, *81*, 799. (c) Liptay, W. *Dipole Moments and Polarizabilities of Molecules in Excited Electronic States*; Academic Press: New York, 1974; Vol. 1. (d) Lippert, E.; Lüder, W.; Moll, F.; Nägele, W.; Boos, H.; Prigge, H.; Seibold-Blankenstein, I. *Angew. Chem.* **1961**, *73*, 695.
(96) (a) Gryczinski, I.; Kawski, A.; Gryczynski, Z.; Gloyna, D. *J. Chem. Soc., Faraday Trans. 2*, **1986**, *82*, 1879. (b) Kobayashi, T.; Ohtani, H.; Kurokowa, K. *Chem. Phys. Lett.* **1985**, *121*, 356.
(97) (a) Hynes, J. T. *Annu. Rev. Phys. Chem.* **1985**, *36*, 573. (b) Hynes, J. T. *J. Stat. Phys.* **1986**, *42*, 149. (c) Hynes, J. T. *Theory of Chemical Reactions*; CRC, New York, 1985; Vol. IV.
(98) Nitzan, A. *Advances in Chemical Physics*; Wiley: New York, 1988; Vol. 70, p 489.
(99) Berne, B. J.; Borkevec, M.; Straub, J. E. *J. Phys. Chem.* **1988**, *92*, 3711.
(100) Hänggi, P.; Talkner, T.; Borkovec, M. *Rev. Mod. Phys.* **1990**, *62*, 251.
(101) Edelman, S. A. *J. Stat. Phys.* **1986**, *42*, 37.
(102) (a) Ladanyi, B. M.; Evans, G. T. *J. Chem. Phys.* **1983**, *79*, 944. (b) Knauss, D. C.; Evans, G. T. *J. Chem. Phys.* **1981**, *74*, 4627.
(103) (a) Villaeys, A. A.; Boeglin, A.; Lin, S. H. *J. Chem. Phys.* **1985**, *82*, 4044. (b) Villaeys, A. A.; Boeglin, A.; Lin, S. H. *Chem. Phys. Lett.* **1985**, *116*, 210.
(104) Johnston, H. S. *Gas Phase Reaction Rate Theory*; Ronald Press: New York, 1966.
(105) (a) Wardlaw, D. M.; Marcus, R. A. *Advances in Chemical Physics*; Wiley: New York, 1988; Vol. 70, p 231. (b) Troe, J. *Physical Chemistry: An Advanced Treatise*; Academic: New York, 1975.
(106) (a) Schroeder, J.; Troe, J. *Annu. Rev. Phys. Chem.* **1987**, *38*, 163. (b) Troe, J. *J. Phys. Chem.* **1986**, *90*, 357. (c) Gehrke, C.; Schroeder, J.; Troe, J.; Voss, F. *J. Chem. Phys.* **1990**, *92*, 4805.
(107) (a) Hasha, D. L.; Eguchi, T.; Jonas, J. *J. Chem. Phys.* **1981**, *75*, 1571. (b) *Ibid. J. Am. Chem. Soc.* **1982**, *104*, 2290; Jonas, J. *Acc. Chem. Res.* **1984**, *17*, 74. (c) Kuharski, R. A.; Chandler, D.; Montgomery, J. A., Jr.; Rabii, F.; Singer, S. J. *J. Phys. Chem.* **1988**, *92*, 3261. (d) Singer, S. J.; Kuharski, R. A.; Chandler, D. *J. Phys. Chem.* **1986**, *90*, 6015.
(108) (a) Courtney, S. H.; Fleming, G. R. *Chem. Phys. Lett.* **1984**, *103*, 443. (b) Courtney, S. H.; Fleming, G. R. *J. Chem. Phys.* **1985**, *83*, 215.
(109) (a) Maneke, G.; Schroeder, J.; Troe, J.; Voss, F. *Ber. Bunsen.-Ges. Phys. Chem.* **1985**, *89*, 896. (b) Schroeder, J.; Schwarzer, D.; Troe, J.; Voss, F. *J. Chem. Phys.* **1990**, *93*, 2393.
(110) Lee, M.; Holtom, G. R.; Hochstrasser, R. M. *Chem. Phys. Lett.* **1985**, *118*, 359.
(111) Kramers, H. A. *Physica* **1940**, *7*, 284.
(112) (a) Chandrasekhar, S. *Rev. Mod. Phys.* **1943**, *15*, 1. (b) McQuarrie, D. A. *Statistical Mechanics*; Harper and Row: New York, 1973.
(113) (a) Montgomery, J. A., Jr.; Chandler, D.; Berne, B. *J. Chem. Phys.* **1979**, *70*, 4056. (b) Montgomery, J. A., Jr.; Holmgren, S. L.; Chandler, D. *J. Chem. Phys.* **1980**, *73*, 3688.
(114) (a) Skinner, J. L.; Wolynes, P. G. *J. Chem. Phys.* **1978**, *69*, 2143. (b) Garrity, D. K.; Skinner, J. L. *Chem. Phys. Lett.* **1983**, *95*, 46.
(115) (a) Grote, R. F.; Hynes, J. T. *J. Chem. Phys.* **1981**, *74*, 4465. (b) Grote, R. F.; Hynes, J. T. *J. Chem. Phys.* **1982**, *77*, 3370.
(116) (a) Carmeli, B.; Nitzan, A. *Chem. Phys. Lett.* **1984**, *106*, 329. (b) Carmeli, B.; Nitzan, A. *Phys. Rev. Lett.* **1983**, *51*, 233.
(117) (a) Borkovec, M.; Berne, B. J. *J. Chem. Phys.* **1985**, *82*, 794. (b) Straub, J. E.; Borkovec, M.; Berne, B. J. *J. Chem. Phys.* **1986**, *84*, 1788.
(118) (a) Okuyama, S.; Oxtoby, D. W. *J. Chem. Phys.* **1986**, *84*, 5830. (b) Pollak, E.; Grabert, H.; Hanggi, P. *J. Chem. Phys.* **1989**, *91*, 4073. (c) Dygas, M. M.; Matkowsky, B. J.; Schuss, Z. *J. Chem. Phys.* **1985**, *83*, 597. (d) Pollak, E. *J. Chem. Phys.* **1987**, *86*, 3944. (e) Schlitter, J. *Chem. Phys.* **1988**, *120*, 187. (f) Adelman, S. A. *J. Stat. Phys.* **1986**, *42*, 37.
(119) Grote, R. F.; Hynes, J. T. *J. Chem. Phys.* **1980**, *73*, 2715. (b) *Ibid.* **1981**, *74*, 4465.
(120) Zeglinski, D. M.; Waldeck, D. H. *J. Phys. Chem.* **1988**, *92*, 692.
(121) Patterson, G. D.; Carroll, P. J. *J. Phys. Chem.* **1985**, *89*, 1344 and references therein.
(122) Herzfeld, K. F.; Litovitz, T. A. *Absorption and Dispersion of Ultrasonic Waves*; Academic: New York, 1959.
(123) (a) Lee, J.; Zhu, S. B.; Robinson, G. W. *J. Phys. Chem.* **1987**, *91*, 4273. (b) Zhu, S. B.; Lee, J.; Robinson, G. W.; Lin, S. H. *Chem. Phys. Lett.* **1988**, *148*, 164.
(124) (a) Zhu, S. B.; Lee, J.; Robinson, G. W. *J. Phys. Chem.* **1988**, *92*, 2401. (b) Zhu, S. B.; Lee, J.; Robinson, G. W. *J. Chem. Phys.* **1988**, *88*, 7088. (c) Zhu, S. B.; Lee, J.; Robinson, G. W.; Lin, S. H. *J. Chem. Phys.* **1989**, *90*, 6335. (d) Zhu, S. B.; Singh, S.; Robinson, G. W. *Phys. Rev. A* **1989**, *40*, 1109.
(125) Velsko, S. P.; Waldeck, D. H.; Fleming, G. R. *J. Chem. Phys.* **1983**, *78*, 249.
(126) Sun, Y. P.; Saltiel, J. *J. Phys. Chem.* **1989**, *93*, 8310.
(127) (a) Bowman, R. M.; Eisenthal, K. B. *Chem. Phys. Lett.* **1989**, *155*, 99. (b) Bowman, R. M.; Eisenthal, K. B.; Millar, D. P. *J. Chem. Phys.* **1988**, *89*, 762.
(128) Lee, M.; Haseltine, J. N.; Smith, A. B., III; Hochstrasser, R. M. *J. Am. Chem. Soc.* **1989**, *111*, 5044.
(129) (a) Bagchi, B. *Int. Rev. Phys. Chem.* **1987**, *6*, 1. (b) Bagchi, B.; Oxtoby, D. *J. Chem. Phys.* **1983**, *78*, 2735.
(130) Xie, C. L.; Campbell, D.; Jonas, J. *J. Chem. Phys.* **1990**, *92*, 3736.
(131) (a) Lee, S.; Karplus, M. *J. Phys. Chem.* **1988**, *92*, 1075. (b) Larson, R. S.; Kostin, M. D. *J. Chem. Phys.* **1982**, *77*, 5017. (c) Berezhkovskii, A. M.; Berezhkovskii, L. M.; Zitzerman, V. Y. *Chem. Phys.* **1989**, *130*, 55. (d) Matkowsky, B. J.; Nitzan,

A.; Schuss, Z. *J. Chem. Phys.* **1988**, *88*, 4765. (e) Klosek-Dygas, M. M.; Hoffman, B. M.; Matkowsky, B. J.; Nitzan, A.; Ratner, M. A.; Schuss, Z. *J. Chem. Phys.* **1989**, *90*, 1141. (f) Pollak, E. *J. Chem. Phys.* **1990**, *93*, 1116.
(132) (a) Agmon, N.; Hopfield, J. J. *J. Chem. Phys.* **1983**, *78*, 6947. (b) *Ibid.* **1983**, *79*, 2042. (c) Agmon, N.; Kosloff, R. *J. Phys. Chem.* **1987**, *91*, 1988.
(133) (a) Sumi, H.; Marcus, R. A. *J. Chem. Phys.* **1986**, *84*, 4272. (b) *Ibid.* 4894. (c) Nadler, W.; Marcus, R. A. *J. Chem. Phys.* **1987**, *86*, 3906. (d) *Ibid. Israel J. Chem.* **1990**, *30*, 69.
(134) (a) Kaufman, A. D.; Whaley, K. B. *J. Chem. Phys.* **1989**, *90*, 2758. (b) Chen, D. H.; Coalson, R. C., unpublished results.
(135) Bagchi, B.; Fleming, G. R. *J. Phys. Chem.* **1990**, *94*, 9.
(136) Agmon, N.; Rabinovich, S., submitted for publication in *J. Phys. Chem.*
(137) (a) van der Zwan, G.; Hynes, J. T. *Chem. Phys.* **1984**, *90*, 21. (b) van der Zwan, G.; Hynes, J. T. *J. Chem. Phys.* **1983**, *78*, 4174. (c) *Ibid. Chem. Phys. Lett.* **1983**, *101*, 367.
(138) (a) Smedartchina, Z. *Chem. Phys. Lett.* **1985**, *113*, 307. (b) Yan, Y.; Sparpaglione, M.; Mukamel, S. *J. Phys. Chem.* **1988**, *92*, 4842.
(139) (a) Moro, G. J.; Nordio, P. L.; Polimeno, A. *Mol. Phys.* **1989**, *68*, 1131. (b) Giacometti, G.; Moro, G. J.; Nordio, P. L.; Polimeno, A. *J. Mol. Liq.* **1989**, *42*, 19.
(140) Zusman, L. D. *Chem. Phys.* **1990**, *144*.
(141) (a) Park, N. S.; Waldeck, D. H. *J. Phys. Chem.* **1990**, *94*, 662. (b) Sivakumar, N.; Hoburg, E. A.; Waldeck, D. H. *J. Chem. Phys.* **1989**, *90*, 2305.
(142) (a) Syage, J. A.; Felker, P. M.; Zewail, A. H. *J. Chem. Phys.* **1984**, *81*, 4706. (b) Felker, P. M.; Zewail, A. H. *J. Phys. Chem.* **1985**, *89*, 5402. (c) Syage, J. A.; Lambert, W. R.; Felker, P. M.; Zewail, A. H.; Hochstrasser, R. M. *Chem. Phys. Lett.* **1982**, *88*, 266.
(143) (a) Troe, J.; Schroeder, J. *J. Phys. Chem.* **1986**, *90*, 4215. (b) Troe, J. *Chem. Phys. Lett.* **1985**, *114*, 241.
(144) (a) Majors, T. J.; Even, U.; Jortner, J. *J. Chem. Phys.* **1984**, *81*, 2330. (b) Amirav, A.; Jortner, J. *Chem. Phys. Lett.* **1983**, *95*, 295.
(145) Felker, P. M.; Lambert, W. R.; Zewail, A. H. *J. Chem. Phys.* **1985**, *82*, 3003.
(146) (a) Bain, A. J.; McCarthy, P. J.; Hochstrasser, R. M. *Chem. Phys. Lett.* **1986**, *125*, 307. (b) Negus, D. K.; Green, D. S.; Hochstrasser, R. M. *Chem. Phys. Lett.* **1985**, *117*, 409.
(147) Myers, A. B.; Holt, P. L.; Pereira, M. A.; Hochstrasser, R. M. *Chem. Phys. Lett.* **1986**, *132*, 585.
(148) (a) Scherer, N. F.; Perry, J. W.; Doany, F. E.; Zewail, A. H. *J. Phys. Chem.* **1985**, *89*, 894. (b) Perry, J. W.; Scherer, N. F.; Zewail, A. H. *Chem. Phys. Lett.* **1983**, *103*, 1. (c) Scherer, N. F.; Khundkar, L. R.; Rose, T. S.; Zewail, A. H. *J. Phys. Chem.* **1987**, *91*, 6478.
(149) Rademann, K.; Even, U.; Rozen, S.; Jortner, J. *Chem. Phys. Lett.* **1986**, *125*, 5.
(150) Fleming, G. R.; Courtney, S. H.; Balk, M. W. *J. Stat. Phys.* **1986**, *42*, 83.
(151) Balk, M. W.; Fleming, G. R. *J. Phys. Chem.* **1986**, *90*, 3975.
(152) Schroeder, J.; Troe, J. *Chem. Phys. Lett.* **1985**, *116*, 453.
(153) Kim, S. K.; Fleming, G. R. *J. Phys. Chem.* **1988**, *92*, 2168.
(154) Park, N. S.; Waldeck, D. H. *J. Chem. Phys.* **1989**, *91*, 943.
(155) Saltiel, J.; Sun, Y. P. *J. Phys. Chem.* **1989**, *93*, 6246.
(156) Sumitani, M.; Nakashima, N.; Yoshihara, K.; Nagakura, S. *Chem. Phys. Lett.* **1977**, *51*, 183.
(157) Sundstrom, V.; Gillbro, T. *Ber. Bunsen.-Ges. Phys. Chem.* **1985**, *89*, 222.
(158) Good, H. P.; Wild, U. P.; Haas, E.; Fischer, E.; Resewitz, E. P.; Lippert, E. *Ber. Bunsen.-Ges. Phys. Chem.* **1982**, *86*, 126.
(159) Taylor, J. R.; Adams, M. C.; Sibbett, W. *Appl. Phys. Lett.* **1979**, *35*, 590.
(160) Rothenberger, G.; Negus, D. K.; Hochstrasser, R. M. *J. Chem. Phys.* **1983**, *79*, 5360.
(161) Heisel, F.; Miehe, J. A.; Sipp, B. *Chem. Phys. Lett.* **1979**, *61*, 115.
(162) Smit, K. J.; Ghiggino, K. P. *Chem. Phys. Lett.* **1985**, *122*, 369. (b) *Ibid. J. Photochem.* **1986**, *34*, 23. (c) Smit, K. J.; Ghiggino, K. P. *Dyes Pigm.* **1987**, *8*, 83.
(163) (a) Sundstrom, V.; Gillbro, T. *Chem. Phys. Lett.* **1984**, *109*, 538. (b) Akesson, E.; Bergstrom, H.; Sundstrom, V.; Gillbro, T. *Chem. Phys. Lett.* **1986**, *126*, 385.
(164) Hicks, J. M.; Vandersall, M. T.; Sitzmann, E. V.; Eisenthal, K. B. *Chem. Phys. Lett.* **1987**, *135*, 413.
(165) Kim, S. K.; Courtney, S. H.; Fleming, G. R. *Chem. Phys. Lett.* **1989**, *159*, 543.
(166) Sun, Y. P.; Saltiel, J.; Hoburg, E. A.; Park, N. S.; Waldeck, D. H., in preparation.
(167) Hoburg, E. A.; Waldeck, D. H., unpublished results.
(168) Ben-Amotz, D.; Drake, J. M. *J. Chem. Phys.* **1988**, *89*, 1019 and references therein.
(169) Spernol, A.; Wirtz, K. *Z. Naturforsch. A* **1952**, *8*, 522.
(170) Dote, J. L.; Kivelson, D.; Schwartz, R. N. *J. Phys. Chem.* **1981**, *85*, 2169.
(171) (a) Doolittle, A. K. *J. Appl. Phys.* **1951**, *22*, 1471. (b) Grest, G. S.; Cohen, M. H. *Adv. Chem. Phys.* **1981**, *48*, 45.
(172) Kunjappu, J. T.; Rao, K. N. *Ind. J. Chem.* **1987**, *26A*, 636.
(173) (a) Castner, E. W., Jr.; Maroncelli, M.; Fleming, G. R. *J. Chem. Phys.* **1987**, *86*, 1090. (b) Castner, E. W., Jr.; Fleming, G. R.; Bagchi, B.; Maroncelli, M. *J. Chem. Phys.* **1988**, *89*, 3519. (c) Maroncelli, M.; Fleming, G. R. *J. Chem. Phys.* **1988**, *89*, 875. (d) Simon, J. D.; Su, S. G. *J. Phys. Chem.* **1988**, *92*, 2368. (e) Simon, J. D. *Acc. Chem. Res.* **1988**, *21*, 128.
(174) (a) Nagarajan, V.; Brearley, A. M.; King, T. J.; Barbara, P. F. *J. Chem. Phys.* **1987**, *86*, 3183. (b) Kahlow, M. A.; Jarzeba, W.; Kang, T. J.; Barbara, P. F. *J. Chem. Phys.* **1989**, *90*, 151. (c) Kahlow, M. A.; Kang, T. J.; Barbara, P. F. *J. Chem. Phys.* **1988**, *88*, 2372.
(175) Safarzadeh-Amiri, A. *Chem. Phys. Lett.* **1986**, *125*, 272.
(176) Negri, F.; Orlandi, G. *J. Phys. Chem.* **1981**, *95*, 748.
(177) Sension, R. J.; Repinec, S. T.; Hochstrasser, R. M. *J. Chem. Phys.* **1990**, *93*, 9185.